July 2019

Tropomyosin-Based Effects of Acidosis on Thin-Filament Regulation During Muscle Fatigue

Brent Scott

TROPOMYOSIN-BASED EFFECTS OF ACIDOSIS ON THIN-FILAMENT REGULATION DURING MUSCLE FATIGUE

A Thesis Presented

By

BRENT DANIEL SCOTT

Submitted to the Graduate School of the
University of Massachusetts Amherst in partial fulfillment
of the requirements for the degree of

Master of Science

May 2019

Department of Kinesiology

TROPOMYOSIN-BASED EFFECTS OF ACIDOSIS ON THIN-FILAMENT REGULATION DURING MUSCLE FATIGUE

A Thesis Presented

by

BRENT DANIEL SCOTT

Approved as to style and content by:

_____

Edward P. Debold, Chair

_____

Becky M. Miller, Member

_____

Jeffrey R. Moore, Member

_____

Jane Kent, Department Head
Kinesiology

ABSTRACT

TROPOMYOSIN-BASED EFFECTS OF ACIDOSIS ON THIN-FILAMENT REGULATION DURING MUSCLE FATIGUE

MAY 2019

BRENT D. SCOTT, B.S., BELMONT UNIVERSITY

M.S., UNIVERSITY OF MASSACHUSETTS AMHERST

Directed by: Professor Edward P. Debold

Skeletal muscle fatigue is defined as a loss in the force/velocity generating capacity of a muscle. A portion of the loss in function is attributable to effects of acidosis (i.e. low pH) on the regulatory proteins, troponin and tropomyosin (Tm), which regulate the binding of myosin and actin in a calcium (Ca^{++}) dependent manner. However, the relative role of troponin and Tm on myosin-actin function during acidosis is not clear, nor are the mechanisms underlying these effects. **PURPOSE:** To determine the role of Tm in the acidosis-induced depression of muscle function using isolated muscle proteins in an in vitro motility assay. **METHODS:** Three mutant constructs of Tm were expressed by replacing the two amino acid (histidine) residues most likely affected by low pH with alanine residues (H153A, H276A, H153A/H276A). These mutant constructs were compared to wild-type Tm (wt-Tm) in order to test whether the acidosis-induced charge change of the histidine amino acid governs the pH-dependent alteration of tropomyosin and therefore the decrease in maximal RTF velocity and Ca^{++}-sensitivity. The effect of acidosis on regulated thin filament (RTF) function was determined by assessing the impact of low pH (pH 6.8) versus neutral pH (pH 7.4) on myosin's ability to move RTFs in the motility assay as a function of increasing levels of Ca^{++}. This was done separately

for the wt-Tm and each structural variant. **RESULTS:** A two-way ANOVA (pH x Tm construct) revealed that acidosis significantly ($p<0.05$) depressed the maximal sliding velocity of the RTFs across all versions of Tm, but that the magnitude of the depression was similar among the wt and all of the Tm mutants. Acidosis did not significantly depress the sensitivity to Ca^{++} under the unloaded conditions of this assay ($p>0.05$). **CONCLUSIONS:** These data suggest that the histidine residues in tropomyosin do not mediate the acidosis-induced depression in contraction velocity observed during muscle fatigue. However, since these residues may be more important in mediating the depression of force, we are currently testing the impact of the three mutant Tm constructs on the acidosis-induced depression in Ca^{++}-sensitivity using a loaded in vitro motility assay.

TABLE OF CONTENTS

Page

LIST OF TABLES

Table Page

LIST OF FIGURES

Figure Page

CHAPTER 1

INTRODUCTION

1.1 – The Importance of Understanding Skeletal Muscle Fatigue

Skeletal muscle fatigue is the decrease in the maximum force or power generating capacity of a muscle in response to repeated stimulation (37) and has both performance and clinical implications. Athletic performance is limited by the muscle's ability to function normally after prolonged use and maximal exertion, but more importantly fatigue is a common disease symptom affecting patients' ability to complete normal activities of daily living and live independently, subsequently decreasing their quality of life. In fact, skeletal muscle fatigue has been identified as an early predictor for and hallmark symptom of chronic heart disease (15, 16, 58). Considering heart disease is the leading cause of death in the U.S. (56), it becomes evident that there is a high prevalence of patients suffering from symptoms of skeletal muscle fatigue. While metabolic acidosis has been identified as a putative fatiguing agent (19) it remains unclear how acidosis affects the molecular regulation of muscle function that leads to the overall decrease in muscular performance.

1.2 – The Problem is in the Muscle

Muscle fatigue is an extremely complex issue that can result from a disruption in central nervous stimulation to the muscle, or as a result of local metabolic perturbations affecting the contractile components of the muscle (9, 12). Seminal research by early muscle physiologists provide strong evidence that factors of fatigue reside within the muscle itself (52). In fact, it has been suggested that 80% of the overall effects of fatigue are due to the local effects on the contractile components (36). There are multiple

fatiguing factors thought to be at play locally in the muscle that work in conjunction to depress muscle function during fatigue. Of those, acidosis is thought to have significant impact as whole muscle studies using magnetic resonance spectroscopy have identified an ***association*** between fatigue and acidosis (38), and single muscle fiber experiments confirm and establish ***causal link*** between the two (6, 39). The resulting effects of acidosis on the muscle are a small decrease in maximal isometric force, a large decrease in unloaded contraction velocity, and a substantial decrease of the calcium sensitivity (21, 39, 57). Coupling these events together result in less force and velocity at the same Ca^{2+} concentration (Figure 1.1).

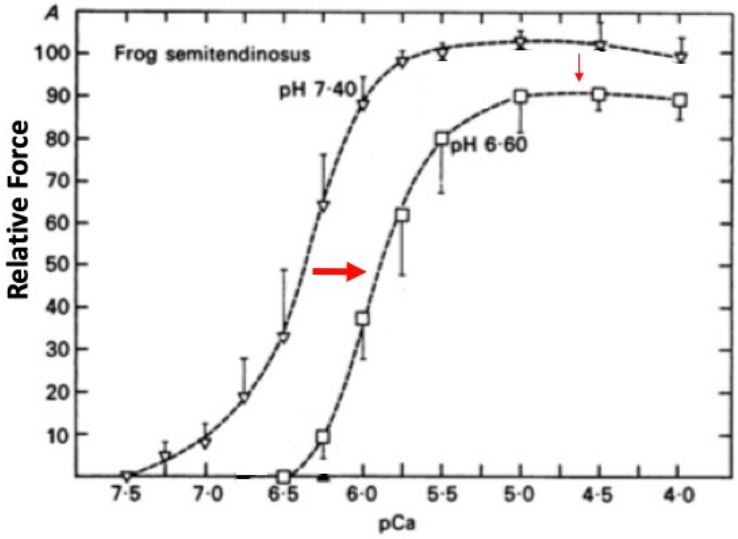

Figure 1.1: The effects of acidosis on the force-pCa curve from single muscle fibers. Down arrow represents the effects of acidosis on myosin. The right arrow indicates the effects on Ca^{2+}-sensitivity – it takes more stimulation (and energy) to generate the same relative force during acidosis. Adapted from Fabiato & Fabiato 1978.

The goals of recent work have been to identify the steps in the cross-bridge cycle that are affected by pH changes as well as to investigate the role of the regulatory proteins during fatigue-induced acidosis (10, 12). However, despite these recent efforts

the complete effects of acidosis on the Ca^{2+} sensitivity of muscle remains unknown. The focus of this study was on the depression in calcium activation observed with acidosis and more particularly on investigating a mechanism underlying the rightward shift in the pCa curve as shown in Figure 1. A part of this calcium insensitivity can be attributed to a decrease in the amount of Ca^{2+} released from the sarcoplasmic reticulum (1) or to a decrease in troponin's Ca^{2+} affinity (61), but there is also evidence that tropomyosin has a role since Tm mediates the pH dependence of active tension in single muscle fibers (20). This study by Fujita & Ishiwata (1999) suggests tropomyosin has a significant role in determining the effects of acidosis on a muscle's activation. However, the underlying molecular mechanisms responsible for tropomyosin's role during the depressive effects of acidosis remain unknown. The goal of this study was to identify a molecular mechanism and Tm's role in the acidosis-induced depression in Ca^{2+}-sensitivity.

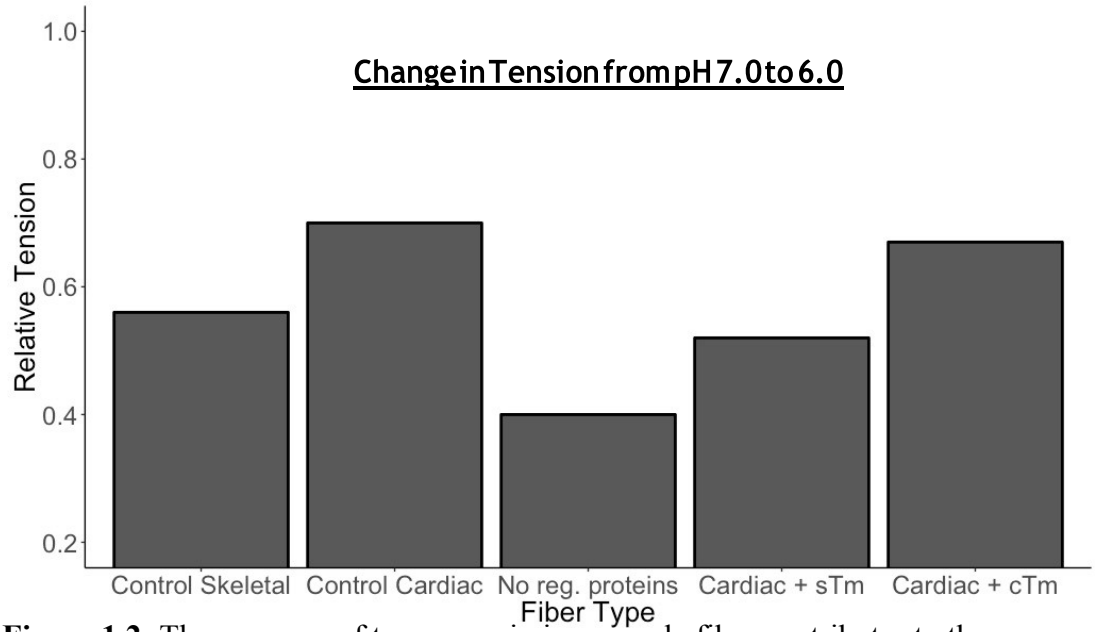

Figure 1.2: The presence of tropomyosin in a muscle fiber contributes to the effects of acidosis on a muscle fiber. Bars represent relative tension produced at pH 6.0 in control skeletal and cardiac fibers, cardiac fibers with actin only, and cardiac fibers with actin and skeletal or cardiac tropomyosin (sTm or cTm). Representative data from Fujita & Ishiwata (1999).

CHAPTER 2

LITERATURE REVIEW

2.1 – Regulation of Muscle Activation

Tropomyosin's functional role as a sarcomere protein is to aid in the local regulation of muscle activation. While there is a cascade of highly coordinated events that need to occur within the neuromuscular system to allow any human movement to occur, the scope of this proposal is on tropomyosin and its role in regulating actomyosin interaction. Consequently, this literature review was focused on tropomyosin's structure and function as it relates to regulating actomyosin interactions.

The actin filament is decorated with regulatory proteins, troponin and tropomyosin, that work in conjunction with one another to regulate muscle contraction. Tropomyosin (Tm) is a long coiled-coiled protein that lies on the surface of actin and serves as the gate-keeper to control actomyosin interactions. Its position on actin is governed by both troponin and myosin which bias Tm into positions that either prevent or promote myosin binding. However, Tm does not exist as a binary on/off switch, but instead has a three-state equilibrium and is activated via a highly cooperative process (49).

There are four different states Tm has been identified as occupying on the surface of actin. Three of them correspond to functional states Tm can reside in as it regulates actomyosin binding. These are termed "blocked-state", "closed-state", and "open-state". The fourth state indicates the position of isolated Tm on the surface of actin without the biasing influence of troponin or myosin, termed "apo" (i.e. Greek for "free from") (66). When incorporated into a thin filament on actin, the presence of troponin constrains Tm

into its "blocked-state" when no Ca^{2+} is present. This state prevents exposure of myosin binding sites on actin and prevents any actomyosin interactions from occurring. Troponin is a three sub-unit complex that consists of a Ca^{2+} binding region (TnC), a tropomyosin binding unit (TnT), and an inhibitory unit (TnI) that attaches to actin and this is responsible for constraining Tm in the "blocked-state" in the absence of Ca^{2+}. When Ca^{2+} binds to troponin it creates an intramolecular reaction within troponin that causes TnI to release actin in favor of a hydrophobic bond with TnC and leaves Tm free from the constrain of troponin (Figure 2.1).

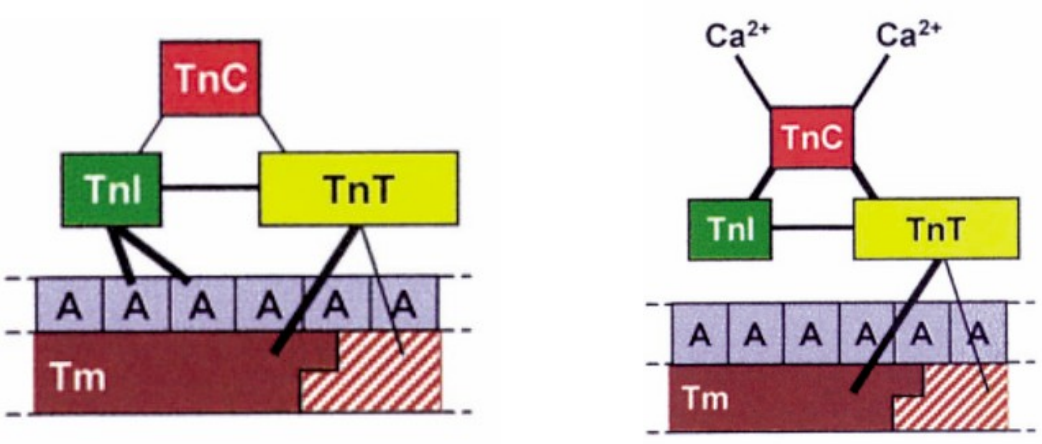

Figure 2.1: Schematic of Tn and Tm interaction and the changes induced by Ca^{2+} binding allowing for movement of Tm over actin. Blue "A" boxes represent actin monomers. The two different Tm colors represent two different Tm molecules. From Gordon et al. 2001.

When TnI releases Tm it is free to explore the surface of actin and moves to the "closed-state" which is in close proximity to its apo state. In the "closed-state", there is partial exposure of myosin binding sites on actin and increases myosin's binding rate 50-fold

(46). Upon the initial formation of actomyosin bonds, the myosin head pushes Tm to its "open-state" which results in fully exposed myosin strong binding sites. Since Tm polymerizes in a head-to-tail overlap it creates a continuous cable that assists in accelerating neighboring myosin heads to bind up to 400 nm from the initial binding location (46). This three state model of Tm is depicted in Figure 2.3 (23). Biochemical solution studies have quantified the amount of time that Tm spends in each of its three unique dynamic equilibrium states under both no Ca^{2+} and saturating Ca^{2+} levels. Briefly, with no Ca^{2+} tropomyosin spends 95% of time in the "blocked-state" and less than 5% of time in either the "closed-state" or "open-state". Under saturating Ca^{2+} conditions, Tm's average time share between states is shifted and Tm spends 70-80% in the "closed-state" and 20-30% in the "open-state" (49).

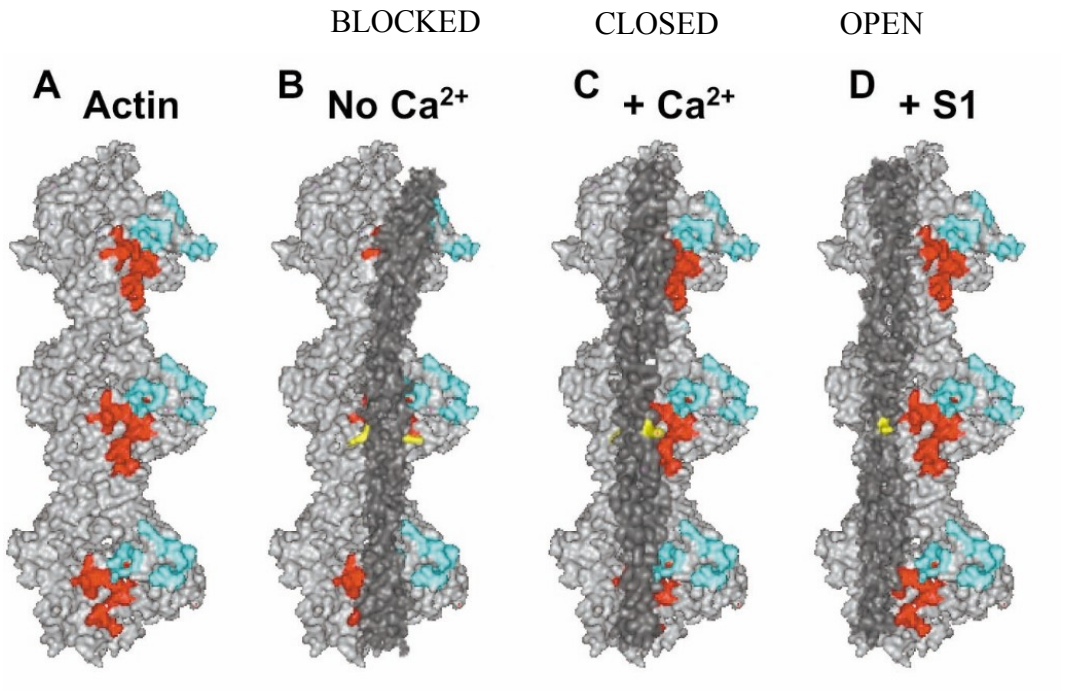

Figure 2.2: Tm three state model. Light gray = actin, dark grey = Tm, blue = weak myosin binding sites, red = strong myosin binding sites. "A" shows actin and myosin binding sites without Tm. Adapted from Gordon et al. 2001.

2.2 – The Role of Electrostatic Interactions in Tm

The structure and interactions of the molecular muscle proteins, and ultimately their functions are governed by electrostatic interactions. For Tm, its position on actin is loosely held in place by sparse, weak electrostatic interactions. There is also a role for electrostatic interactions in the stability of the Tm coil structure. Since an amino acids overall charge is dependent upon the pH of the cellular environment, these basic electrostatic interactions are susceptible to exercise induced acidosis. The next section of the review will focus on the role of electrostatic interactions in Tm's structure and function to highlight the effects of acidosis-induced amino acid charge change.

2.2.1 – Tm isoforms

The Tm isoform present in a muscle depends on the type of muscle (cardiac, fast skeletal, slow skeletal). In striated muscle, the TPM1 and TPM2 genes encode α and β Tm isoforms (63). These two Tm isoforms can dimerize in the form of alpha-alpha (α_2), alpha-beta (αβ), or beta-beta (β_2). Tm isoforms preferentially arrange into the αβ and α_2 isoforms. Fast muscle has an α:β ratio of about 4:1, whereas slow muscle has an α:β ratio close to 1 (7, 47). Tm is a unique protein in which cardiac muscle expresses the isoform associated with fast muscle (α). While a given muscle type is generally characterized by the α:β ratio, there is a variable distribution of α and β isoforms throughout the muscle. The α and β Tm isoforms have the same amino acid sequence in both cardiac and skeletal muscle (63), and differ from each other by 39 residues, all having the same amino acid classification except for two, giving the beta subunit a slightly more negative charge (47). In the present study we will only be studying α_2 Tm as it is the predominate isoform in fast skeletal muscle.

2.2.2 – Tm structure

Tm is a 42 nm long coiled-coil protein and one subunit spans over seven actin monomers. Tm consists of 284 amino acids and is subdivided into a seven amino acid motif that is repeated throughout the entire amino acid sequence and generally follows the sequence, **hydrophobic – polar – polar - hydrophobic – charged – polar – charged (H-P-P-H-C-P-C)** (Figure 2.4). The "a" and "d" nonpolar positions (usually alanine) make-up the inner core of the Tm molecule and help determine its coiled structure. The acidic "b", "c", and "f" positions are usually charged, most conserved to the outside of the Tm cable, and can interact with the surface of actin (3). The "e" and "g" positions make ionic "e-g" pairs that help stabilize the Tm structure and protect the hydrophobic core from the aqueous solution. This characteristic seven amino acid charge motif is interrupted in a select few locations where an amino acid within the heptad repeat is replaced by one with a different charge characteristic. These non-canonical amino acids have important structural implications for Tm since they impart flexibility allowing Tm the ability to twist and find optimal orientation to the surface of actin (41). Additionally, these non-canonical residues contribute to determining Tm's 423nm persistence length as a monomer (44). This distance would span half of the thin filament if the persistence length is unchanged when polymerized on an actin filament indicating that Tm can behave like a flexible rod allowing for more actomyosin interaction to occur as the result of an initial myosin binding event pushing Tm to the "open-state" (i.e. cooperativity).

A

	a	b	c	d	e	f	g	
1	M	D	A	I	K	K	K	
8	M	Q	M	L	K	L	D	
15	K	E	N	A	L	D	R	
22	A	E	Q	A	E	A	D	
29	K	K	A	A	E	E	R	
36	S	K	Q	L	E	D	E	
43	L	V	A	L	Q	K	K	
50	L	K	G	T	E	D	E	
57	L	D	K	Y	S	E	S	
64	L	K	D	A	Q	E	K	
71	L	E	L	A	D	K	K	
78	A	T	D	D	E	S	E	
85	V	A	S	L	N	R	R	
92	I	Q	L	V	E	E	E	
99	L	D	R	A	Q	E	R	
106	L	A	T	A	L	Q	K	
113	L	E	E	A	E	K	A	
120	A	D	E	S	E	R	G	
127	M	K	V	I	E	S	R	
134	A	Q	K	D	E	E	K	
141	M	E	I	Q	E	I	Q	
148	L	K	E	A	K	H	I	
155	A	E	E	A	D	R	K	
162	Y	E	E	V	A	R	K	
169	L	V	I	I	E	G	D	
176	L	E	R	A	E	E	R	
183	A	E	L	S	E	S	K	
190	C	A	E	L	E	S	E	
197	L	K	T	V	T	N	N	
204	L	K	S	L	E	A	Q	
211	A	E	K	Y	S	Q	K	
218	E	D	K	Y	E	E	E	
225	I	K	V	L	T	D	K	
232	L	K	E	A	E	T	R	
239	A	E	F	A	E	R	S	
246	V	T	K	L	E	K	S	
253	I	D	D	L	E	D	E	
260	L	Y	A	Q	K	L	K	
267	Y	K	A	I	S	E	E	
274	L	D	H	A	L	N	D	
281	M	T	S	I				

B

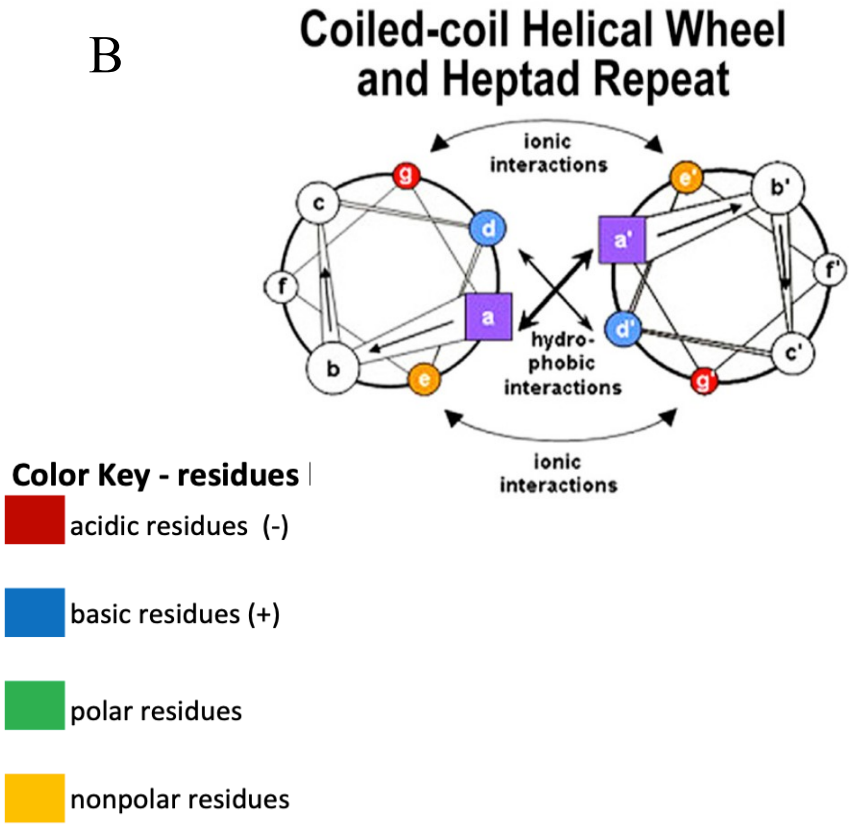

C

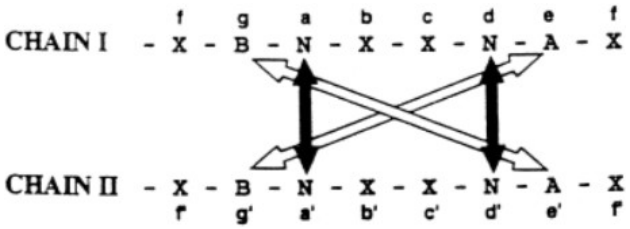

Figure 2.3: Tm's amino acid sequence with known actin binding sites and coiled-coil helical arrangement**.** A) Tm's amino acid sequence in striated chicken muscle. Known residues that contact actin are color coded. B) Cross-sectional view of the arrangement of the coiled-coil structure. C) Relating how the primary structures of each chain would correspond considering the helical organization. White arrows show "e-g" pairs and black arrows indicate "a-d" hydrophobic core interaction. Adapted from Brown & Cohen 2005; Li et al. 2011.

2.2.3 - Tm's pseudo-repeats and interactions with actin

Tm's amino acid sequence is subdivided into seven ~40 amino acid long pseudo-repeats with each pseudo-repeat being further divided into an α-band and β-band (Figure 2.5). Only the amino acids in the α-bands make contact with actin in the "blocked-state", while the β-band residues make contact in the "closed-state" and "open-state" (28, 50, 64). The slight curve in Tm's shape ultimately permits Tm to bind with actin by aligning the seven α-bands that contain acidic residues with the basic residues in actin (45). Figure 2.4 describes Tm's amino acid sequence, organization, and actin binding characteristics (3). Roughly 6% of Tm amino acids are involved in actin binding and the majority of the Tm/actin interaction is from **negatively (-)** charged residues on Tm interacting with **positively (+)** charged residues on the surface of actin. Furthermore, troponin and myosin influence the way in which Tm lies on actin with energy landscapes revealing that Tn constrains Tm in the "blocked-state" in the absence of Ca^{2+}, and that Tm is highly unlikely to achieve its "open-state" without a myosin induced movement (59).

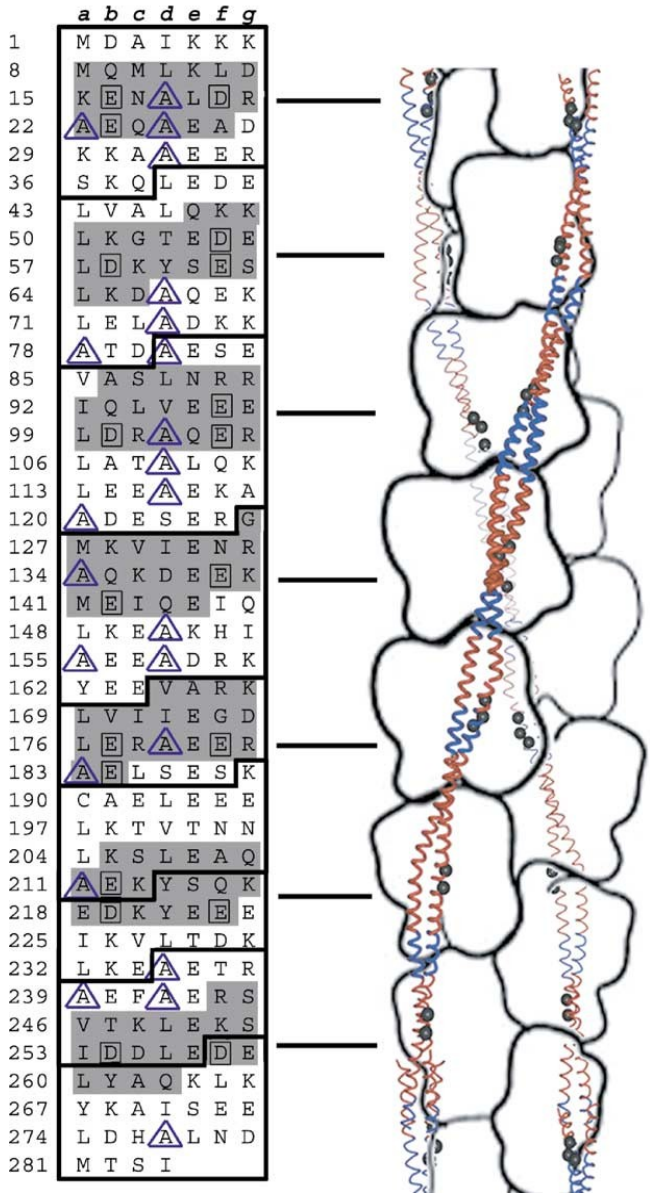

Figure 2.4: Tm primary structure showing actin binding α-band (shaded) and β-band (unshaded). Dark black lines in primary sequence indicate 9 exons that encode the protein. Adapted from Brown & Cohen 2005.

2.2.4 – Tm head-to-tail overlap

Electrostatic interactions are not only involved in Tm's interactions with actin both also in Tm polymerization and stability. Tm polymerization occurs by a head-to-tail overlap with one Tn positioned over this overlap zone. The head-to-tail formation is made from a 10 residue overlap of the N-terminus that fits into the splayed C-terminus that are rotated 90° from each other (Figure 2.6). Most of the intermolecular interactions between the two termini are hydrophobic in nature with ionic interactions occurring intramolecularly which has been suggested to help stabilize the individual Tm chains (25). Additionally, the head-to-tail overlap region is an amino acid sequence that contributes to Tm's overall stability by imparting a rigidity between each Tm molecule (62). A stable connection between Tm molecules is an important for allowing myosin induced "open-state" activation signals to be transmitted throughout the thin filament.

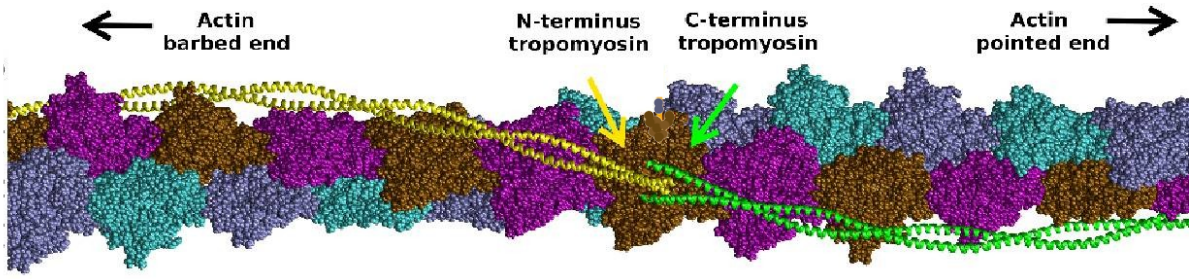

Figure 2.5: Tm head-to-tail overlap models. Two Tm (yellow & green) molecules form a head-to-tail overlap on actin (multi-color spheres). Adapted from Orczechowski et al. 2014.

2.3 – Fatigue-Induced Acidosis: Changes in pH

While there are other fatiguing agents, this study only focuses on the effects caused by acidosis, and consequently it was the only element of fatigue reviewed. The cause of metabolic acidosis has been debated recently and this section will briefly touch on the common explanations. For the purposes related to this study, the fact is that metabolic acidosis does occur. Moreover, the interests of this study are to investigate the effects of acidosis on the contractile proteins regardless of the origins of the increase in H^+ ions that leads to the decreased pH in the muscle.

Fatigue-induced acidosis has been linked to both direct and indirect by-products of ATP hydrolysis when ATP production from oxidative phosphorylation needs to be supplemented with ATP from anaerobic respiratory pathways (34, 67). Historically, the accumulation of the metabolic intermediate, lactate, was suspected to play a major role during muscle fatigue. However, while lactate accumulation is a useful indirect method for measuring fatigue-induced acidosis, it is not itself a fatiguing agent, which is common misconception (34, 67). Rather, the H^+ produced during lactate formation was identified as a potential contributor to the low muscle cell pH leading to fatigue (34). ATP hydrolysis itself was also proposed to provide additional H^+ ions to the cellular environment (67). Regardless, the resulting drop in pH from the increase in H^+ decreases intramuscular pH levels from 7.1 to 6.5 in humans consistently (4, 5, 38).

2.3.1 – pH changes protein surface charge

When the intramuscular pH drops during acidosis it signifies that there is an increased number of H^+ ions in the cellular environment. These protons can not only interfere with the cross-bridge kinetics and calcium dynamics, but also are able to interact

and change the average structural surface charges of the muscle proteins themselves. The Brønsted-Lowry definition of acid/base chemistry denotes the tendency for a substance to donate or receive a proton. The pKa is a measure of the relative strength of an acid or a base that indicates the pH that a substance will lose or gain a proton at. A pH less than the pKa (pH < pKa) indicates a substance will gain a proton from the environment (i.e. protonate). Amino acids' functional groups each have a unique pKa and pH-induced charge change alters the surface charge of a protein when environmental pH changes cause functional groups to gain or lose protons (Figure 2.6).

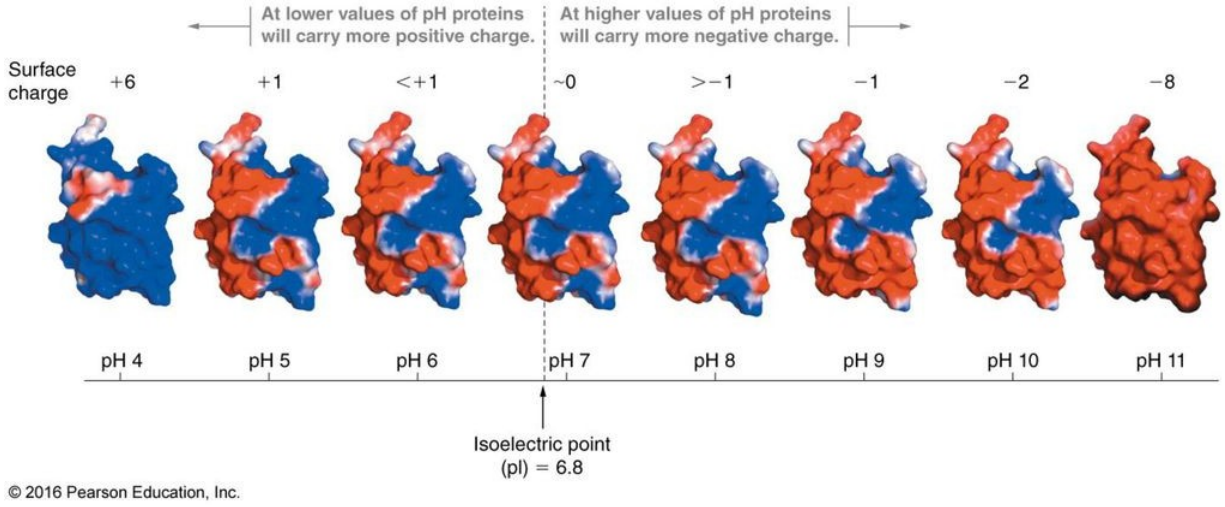

Figure 2.6: Example of pH-induced change of protein surface charge with human ubiquitin. Blue represents positive surface charges and red negative surface charges. As pH is decreased from right to left the protein protonates and the surface charge is increased. From Biochemistry: Concepts and Connections.

Consequently, these charge changes affect the electrostatic interactions that dictate protein structure, interactions, and function. A common example of pH-induced amino acid charge change affecting function is the Bohr Effect that showcases the greater ability for hemoglobin to release oxygen when blood plasma pH decreases. The bicarbonate reaction decreases blood pH that causes the protonation of histidine's (amino acid)

imidazole side chain. This new positive charge added to the side chain creates an intramolecular charge interaction that stabilizes the hemoglobin to an alternate protein form that promotes oxygen release (8).

2.3.2 - Exercise-induced acidosis causes His protonation

Interestingly, histidine is the only amino acid with a side chain pKa within physiological relevancy (pH 6.5) which coincides with intramuscular pH levels observed during exercise-induced acidosis. At resting intramuscular pH levels (pH 7.1), histidine side chains are deprotonated and possess a neutral charge. As intramuscular pH approaches pH 6.5 during acidosis the histidine side chain protonates and changes the residue's overall net charge from neutral to positive (Figure 2.7A). Additionally, a localized micro-environment can change the pKa of an amino acid suggesting that other residues could contribute to pH-induced charge change as well. However, since there are two histidine residues in a single Tm molecule (Figure 2.7B) this study is focused on these specific residues. An acidosis-induced Tm His side chain protonation could change both the intermolecular interactions Tm makes with actin along with the intramolecular interactions Tm makes with itself especially considering the specific location of H276 in the head-to-tail overlap domain (Figure 2.7B). Previous studies show how a single charge change can have a large effect on protein function as single-point mutations on the surface of actin have been shown to change the Tm/actin interaction. The D292V mutation strengthens the Tm/actin interaction and induces a "blocked-state" stabilization (51, 55, 59). The consequences of a "blocked-state" stabilization is a decrease in Ca^{2+}-sensitivity as Tm remains covering myosin binding sites on actin. As a result, the possibility of Tm's His protonation altering Tm function seems plausible since these

single charge changes on the surface of actin can disrupt Tm's position within its dynamic equilibrium.

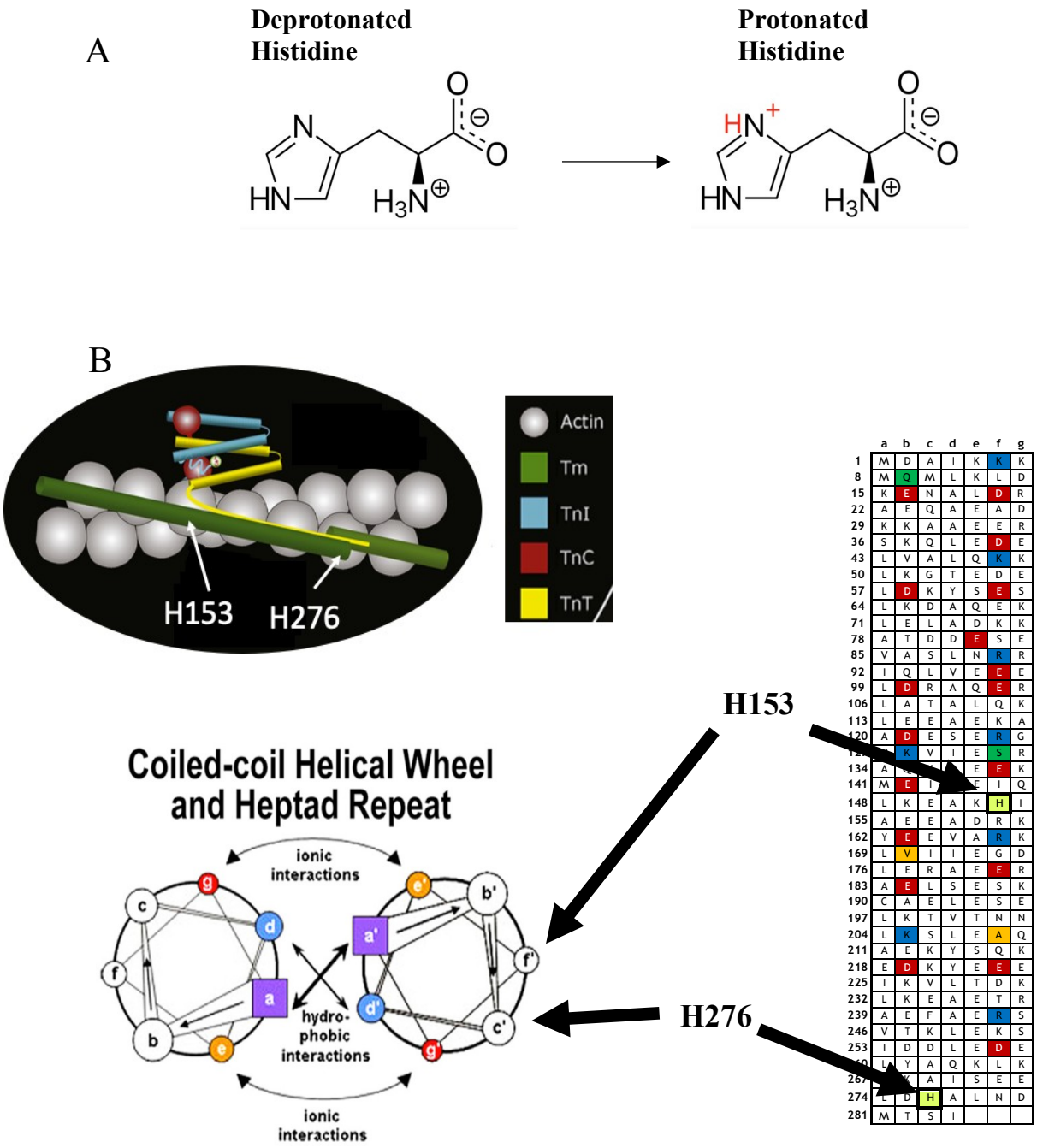

Figure 2.7: Acidosis induced histidine protonation, His location within Tm primary sequence, and position in the heptad repeat A) Histidine gains a positive charge during acidosis. B) Location of His residues in Tm. Top left: General location in Tm relative to the actin/Tm/Tn interface. Right: Precise location of His residues in Tm primary sequence. Bottom left: His position in the Tm coil. The residues face the outside environment allowing them to interact with other Tm resides or proteins. Adapted from Brown & Cohen 2005; Li et al. 2011.

2.3.3 – Henderson-Hasselbach calculations

The Henderson-Hasselbach equation can be used to determine the ratio of protonated to deprotonated His residues at both rest (pH 7.1) and during fatigue (pH 6.5):

1) $pH = pKa + \log_{10}([A^-]/[HA])$

2) $\log_{10}([A^-]/[HA]) = pH - pKa$

3) $[A^-]/[HA] = 10^{pH - pKa}$

pH 7.1: $10^{7.1 - 6.5} = 3.98$

pH 6.5: $10^{6.5-6.5} = 1$

At rest, there is ~4x more deprotonated histidine than protonated, and the slight decrease in pH during fatigue changes the proportion to an equal deprotonated to protonated ratio. These calculations indicate that there has been a large change in histidine protonation that changed the residues from a neutral to positive charge.

2.4 – Specific Aim & Hypothesis

Acidosis depresses the Ca^{2+}-sensitivity of muscle and Tm has been shown to modulate the pH dependent response of muscle during activation. Tm regulates muscle activation by working in conjunction with Tn to sterically block myosin from binding to actin. When Ca^{2+} binds Tn during the initiation of muscle activation Tm is freed to explore other positions on actin. When unconstrained by Tn in the "blocked-state", Tm's position on actin is determined weakly by sparse electrostatic interactions. Not only are electrostatic interactions involved in Tm actin binding, they are also involved in making intramolecular contacts within the Tm molecule. A decrease in pH (i.e. acidosis) can alter the surface charge of a protein altering the structure and changing the protein's function. In physiological relevant pH ranges observed during exercise induced acidosis, histidine

is the only amino acid with a relevant side chain pKa. Histidine's side chain pKa indicates that histidine side chain protonation can occur during skeletal muscle fatigue. There are two His in Tm structure that could change from a neutral to positive charge during acidosis. This charge change could affect the electrostatic interactions Tm makes with actin and itself that could ultimately alter its function. Since the purpose of this study was to find a mechanism underlying Tm's role during the depressive effects of acidosis we have focused in on the effects of Tm's histidine protonation during muscle activation.

2.4.1 – Specific Aim

The aim of this thesis was to determine if histidine removal from Tm affects its ability to regulate actomyosin interactions during acidosis. In a collaboration with the Lab of Dr. Jeffrey Moore we expressed mutant Tm molecules that altered the charge distribution at pH levels associated with fatigue by replacing histidine residues that have physiologically relevant side chain pKas with the neutral, non-protonatable residue, alanine. We examined four different Tm molecules as described in Table 2.1:

Tropomyosin	Mutation	Potential charge changes at low pH
eWT	Control (wild-type)	+2
H153A	Single His at position 153 replaced w/ Ala	+1
H276A	Single His at position 276 replaced w/ Ala	+1
H153A/H276A	Both His replaced w/ Ala	0

Table 2.1: Tm molecules, the mutations performed, and their charge changes at low pH. His: Histidine, Ala: Alanine.

After expression, regulated thin filaments (RTFs) were constructed by reconstituting actin filaments with the expressed Tm variants along with Tn. The RTFs' sliding velocities (V_{RTFs}) were compared with an in vitro motility assay under pH values representing rest (7.4) and fatigue-induced acidosis (6.8) in a variety of different Ca^{2+}concentrations ranging from 10 (absence of Ca^{2+}) to 4 (saturating Ca^{2+}).

2.4.2 - Hypothesis

A location independent removal of a histidine from Tm will exacerbate the effects of pH on V_{RTFs} and the removal of two histidines will decrease V_{RTF} more than a single removal suggesting that the histidine residues attenuate the depressive effects of acidosis by destabilizing the "blocked-state" (Figure 2.10).

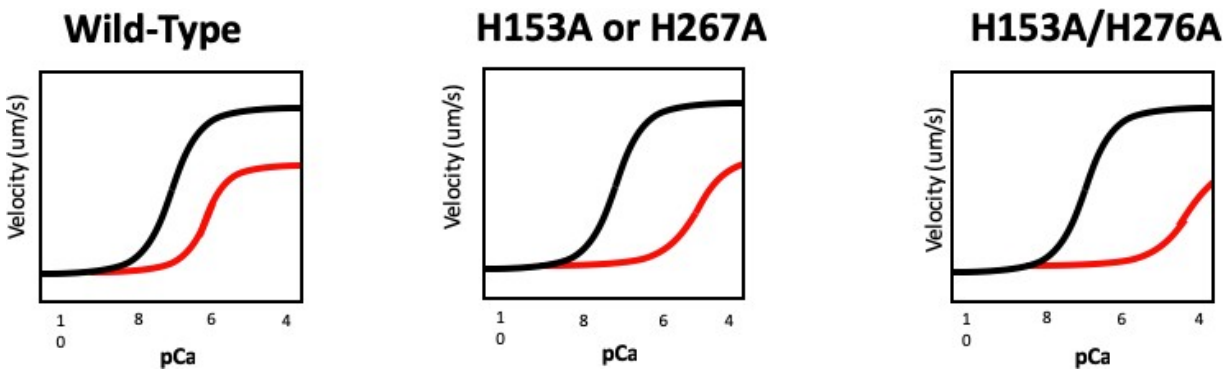

Figure 2.8: Representation of hypothesis – histidine residues help mitigate the depressive effects of acidosis. Velocity measured by in vitro motility. Black lines represent velocity-pCa measured at pH 7.4, and red lines at pH 6.8. No changes expected at pH 7.4. It is predicted one His removal will shift the WT pH 6.8 curve to the right, and the removal of both His residues will further shift the curve to the right.

Hypothesis Rationale:

The hypothesis is His residues in Tm serve as a protective mechanism during exercise-induced acidosis by mitigating the depressive effects of low pH on Ca^{2+}-

sensitivity. The hypothesis is thought to be mediated through His protonation altering Tm's relative position within its dynamic equilibrium as a result of the newly gained positive charges affecting the electrostatic interactions the residues in Tm are involved with. A previous study reported that low pH increases the dissociation temperature of the Tm/actin interaction (71). This result is interpreted as acidosis increasing the Tm/actin affinity in the "blocked-state" under no Ca^{2+} conditions as the presence of troponin constrains Tm in the "blocked-state". During activation when Ca^{2+} binds Tn releasing Tm, the low pH-induced Tm/actin stabilization would slow the movement of Tm out of the "blocked-state" limiting activation; however, the new charges on the His side chain might interfere with the existing electrostatic interactions between Tm and actin weakening them. The effects of His protonation interfering with the Tm/actin interaction counteracts the low pH-induced Tm/actin stabilization and allows Tm to more easily move out of the "blocked-state". Removing the His residues from Tm removes this protective mechanism as there are no residues changing charge to destabilize the "blocked-state". This mechanism seems possible since the location of the H153 residue is in between Glu-142 and Glu-163 which both make contact with basic residues on actin (45). These electrostatic interactions could be directly affected by His protonation if the newly gained positive charge interferes with these interactions. The His charge change could also indirectly alter these interactions by affecting change to the local Tm structure around these residues. This is further evidenced by the results of previous studies on single point actin mutations. These studies suggest a change in surface charge can affect Tm's position within its dynamic equilibrium since the D292V mutation induces a "blocked-state" stabilization (51, 55, 59) when an additional positive charge is added to

actin. Additionally, H276 could also have effects through an alternative mechanism. H276 lies in the C-terminus head-to-tail overlap domain and could alter the polymerization and stability of the Tm polymer since H276 has been shown to form an intramolecular salt bridge with other residues at pH 6.5 (25) and this is an interaction that would not be present under *in vivo* resting conditions (pH 7.1). Furthermore, the experimental protocol allows for the determination for the relative contribution of each histidine residue.

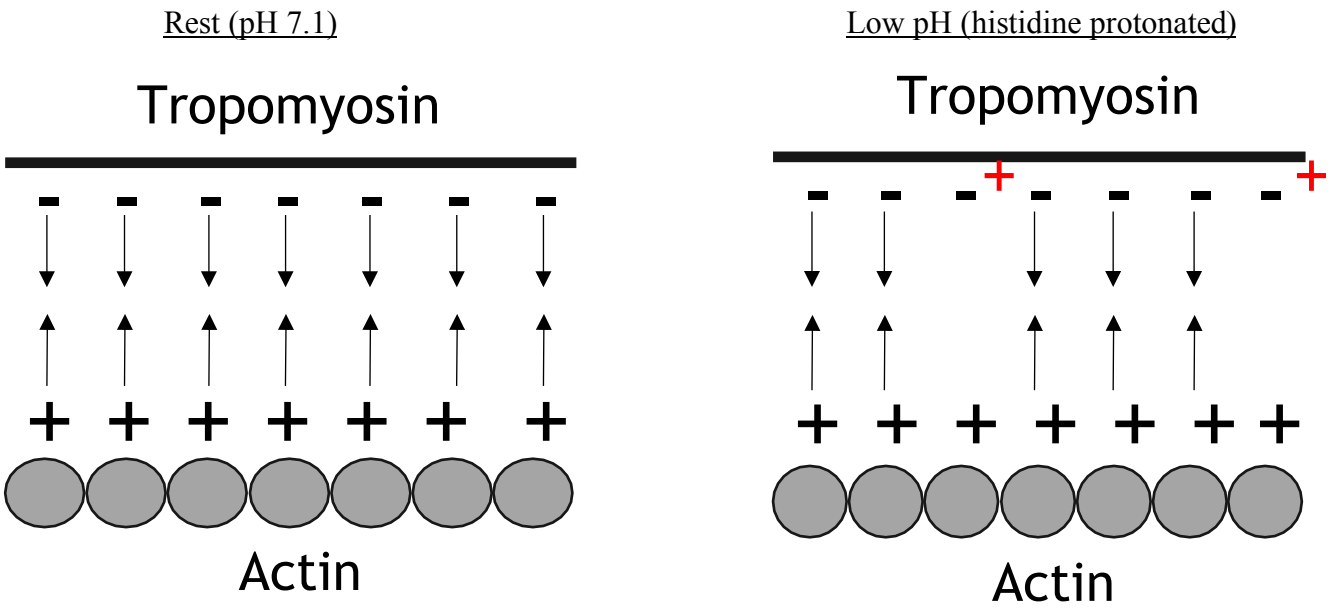

Figure 2.9: Cartoon representation of hypothesis rationale of histidine residues protonation interfering with the Tm/actin interaction that would destabilize the "blocked-state".

CHAPTER 3

METHODS

3.1 – Protein Preparations

3.1.1 – Expression and purification of Tm

The Tm variants used were made using a bacterial system to express α-Tropomyosin from mouse heart RNA in collaboration with the Lab of Dr. Jeff Moore (42). Briefly, cDNA was obtained from the mouse heart RNA using a cDNA synthesis kit and protocol and cloned using a PCR kit. Bacterially expression in E. Coli. was completed using a pET-24 vector system (Novagen, Madison, Wisconsin) as previously described (42). This vector system contains a T7 promotor, lac operator, and kanamycin resistant gene used as a part of the expression of the tropomyosin. Additionally, all bacterially expressed tropomyosin contain Met-Ala-Ser residues added to the N-terminus to mimic the acetylation process that is required for Tm head-to-tail polymerization and subsequent actin binding in bacterially expressed tropomyosin (53). Histidine mutations were added using a site directed mutagenesis kit, and DNA sequencing was performed to verify the presence or absence of histidine residues and the Ala-Ser motif. α-Tm was extracted, purified, and precipitated and stored into final storage buffer containing 50mM KCl, 15mM BES, 4mM $MgCl_2$, and 1mM DTT at pH 7.3. Final protein purity was assessed by SDS PAGE.

3.1.2 – Other proteins

Myosin was purified from chicken pectoralis muscle as described originally by Margossian & Lowey (48), with minor modifications (Debold et al. 2011). Chicken pectoralis muscle is predominately comprised of fast myosin isoform (2). After isolation

and purification, the myosin was stored in glycerol at -20°C, or snap frozen and stored at -80°C. A "deadhead spin down" was performed on the day of experimentation to expel any non-functioning myosin heads (i.e. dead heads). For the spin down 200ug/mL of myosin stock is mixed with 100 ug/mL unlabeled actin, and 1mM ATP for a final volume of 400 uL. Solution was spun at 95,000 RPM for 20 minutes. During the spin, active myosin interacted with actin and cycled through cross-bridge formation while any "deadheads" simply bound to the actin and formed a precipitate. Functioning myosin was pulled from the supernatant and diluted to 100 ug/mL for use in the motility assay.

Actin was isolated and purified as previously described (60) form the same chicken pectoralis muscle. Previous studies report the origin of actin has no effects on sliding velocity in the in vitro motility assay (40). Actin was either kept unlabeled or fluorescently labeled with TRITC/phalloidin (Sigma-Aldrich, St. Louis, MO) as described by Debold et al. (2011) which allowed for visualization under the light microscope.

Purified Troponin ITC complex from fast skeletal from rabbit psoas muscle was purchased from Life Diagnostics (West Chester, PA) aliquoted into 5uL stocks in storage buffer, snap frozen, and stored at -80°C (Debold et al. 2011).

3.2 – Data Collection

3.2.1 – Regulated in vitro motility assay

An in vitro motility assay was used to investigate our hypothesis that removal of histidine exacerbates the effects of acidosis on V_{RTF}, and our aim to find a mechanism underlying Tm's ability to modulate actomyosin interaction under acidic conditions. Motility is a gliding assay where a fix field of myosin on a microscope coverslip propels

actin through solution (Figure 9). The advantage of the motility assay is that it allowed for exact manipulations of the experimental conditions in all aspects: [myosin], [RTF], [ATP], pH, pCa, and temperature. This allowed for effective experimentation simulating fatigue and resting control conditions.

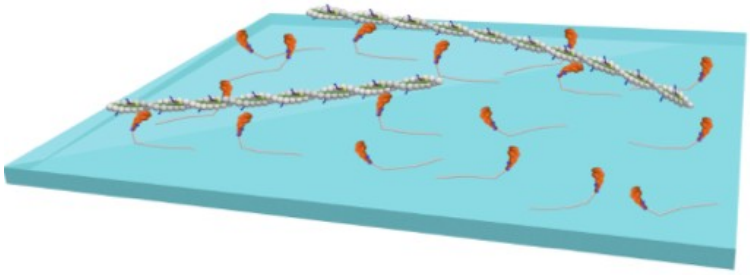

Figure 3.1: Cartoon representation of the regulated in vitro motility assay. Orange myosin are fixed to the coverslip and propel RTF across the surface.

The protocol for the motility preparation was followed as originally described by Kron and Spudich (40) with modifications as previously described by Debold et al. (13, 14). Briefly, 100 ug/mL myosin was injected into the flow cell, allowed to incubate for 30 seconds, and then 0.5 mg/mL BSA (Bovine Serum Albumin, a lipoprotein, i.e. non-actin binding) was flown in to cover the remainder of the surface not inhabited by myosin. This was allowed to incubate for one minute. After, 1 uM unlabeled actin is added that bound to any non-functioning myosin heads to prevent them from acting as a molecular brake during the assay. Following the 30 second incubation of the unlabeled actin coat, 1 mM ATP was introduced and incubated for 30 seconds allowing brief cross-bridge cycling to occur excluding any dead heads bound to the unlabeled actin.

Fluorescently labeled actin was added and incubated for 1 minute, and was free to bind to active myosin, before the addition of the reconstitution solution containing the regulatory proteins. The slide was incubated for 7 minutes before the addition of the final motility buffer containing the desired pH, Ca^{2+}, and ATP. The seven minute reconstitution has been developed and verified as adequate time for reconstitution of RTF using a myosin rigor bond using specific concentrations of actin, Tn, and Tm (29, 31).

3.2.2 – Experimental conditions and equipment

For this thesis, two different pH levels were utilized: 1) 7.4, and 2) 6.8. This modest drop in pH has shown previously to correlate to a 50% reduction in V_{RTF} at pCa 4 (13) and correlates with modest levels of fatigue. Ca^{2+} was assayed at 10, 7, 6.5, 6, 5.5, 5, 4 pCa levels with 10 being the absent of Ca^{2+}. Successful regulation of thin filaments was indicated by no movement of RTFs at pCa 10. There were 4 Tm molecules used to reconstitute the thin filament: 1) WT, 2) H153A, 3) H276A, 4) H153A/H276A.

Once the flow cell was prepped it was transferred to a Nikon Ti-U inverted microscope with a 100X, 1.4 NA CFI Plan Apo oil-coupled objective, and temperature maintained at 30°C. The sliding velocity of the regulated thin filaments (V_{RTF}) were captured with an intensified digital camera (Stanford Photonics, Palo Alto, CA) and frame grabber (Epix, Buffalo Garden, IL) used with PIPER Control software (version 2.5.11, Stanford Photonics). Three to four, 30 seconds videos were captured per slide at different flow cell locations to ensure a variety of sampling variation (considered n=1). These techniques have been validated in detail earlier by Debold et al. (13, 14).

Video analysis was completed with an automated filament-tracking plugin for ImageJ, WRMTRK, a program designed to track and record filament size, velocity, and

total distance travelled. Analysis parameters were set to only include real filament signal and exclude arbitrary bright spot noise or unbound proteins. This included a lower limit for both filament length (0.5 microns), and distance traveled (4 microns over 30sec). This ensured that all movement and velocities recorded are from real actomyosin interactions, and not just filaments floating in solution. RTF filtering was crucial at lower pCa values and helped distinguish between a properly regulated thin filament, and unwanted noise. Each video contained on average 50-100 filaments. The 3-4 videos for each condition average of V_{RTF} on a given day are then averaged together to get the total day V_{RTF} average and considered n=1 for that condition. After each day (n=1) the Hill equation was fit to the data and parameters generated for each condition. Construction of the total final velocity vs pCa curve was complete by averaging each of the day's average so each data point represented the mean velocity of all days with error bars representing between day variation of means. The percent of filaments moving was also calculated from the velocity output data by taking the total number of moving filaments (above lower limit threshold) and divided by the total number of filaments observed.

3.3 – Data Analysis

3.3.1 - Graphing and statistical analysis

Data was plot as velocity-pCa graphs and fit with the Hill equation that generated parameter estimation for the maximal sliding velocity (Vmax), pCa50, and Hill coefficient (n) using SigmaPlot 11.2. The pCa50 and Hillslope parameters provide useful insight into overall calcium sensitivity and degree of cooperativity. The pCa50 and hillslope (n) parameters generated from the fit of the hillslope equation details the calcium concentration that elicits half of the theoretical maximal sliding velocity of the

RTFs (pCa50) and the slope of the curve (n), with an increased slope indicating there is a higher degree of cooperativity exhibited.

The percent of moving filaments was calculated for each recorded video by taking the number of moving filaments and dividing by the total number of filaments (# moving/total), and a filament was considered moving if it moved farther than 4 microns. Data were then plotted against the Ca^{2+} concentration to construct fraction moving – pCa graphs. The resulting scatterplot was curve fit with the Hill equation and the same three parameters V_{max}, pCa_{50}, and hillslope parameters were generated.

Additional statistics were conducted using SigmaPlot 11.2 and R on the fits of Hill equation to each individual experiment day giving multiple values for mean V_{max}, pCa_{50}, and hillslope which can be used as a repeated measure. As a result, a two-way repeated measures ANOVA was performed and was used to identify main effects of both the pH and type of Tm, or any interaction that occurred. Sample size estimation conducted using G*Power 3.1 (18) determined 7-10 experiments per condition is necessary to determine mutant differences on V_{RTF} with an effect size of 1.5, alpha level of 0.05, and power of 0.80. For my hypothesis to hold true, either the max V_{RTF} or pCa_{50} would have to be significantly lower in each of the histidine removal mutants compared to the WT to show that histidine residues help attenuate the depressive effects of acidosis.

CHAPTER 4

RESULTS

4.1 – Velocity results from in vitro motility

Regulated actin filament velocity was measured in an in vitro motility assay (IVM) at two pH levels (7.4 and 6.8) with regulated thin filaments (RTF) reconstituted with four distinct Tm variants. The average velocity recorded at each Ca^{2+} concentration ($[Ca^{2+}]$) from each experimental trial was plotted as a pCa-velocity scatterplot and fit with the Hill equation.

$$\textbf{Hill Equation:} \quad y = \min + \frac{\max - \min}{1 + 10^{(\log EC50 - x)\,\text{Hillslope}}}$$

Fitting data from the in vitro motility (IVM) experiments to the Hill equation generated parameters describing each experimental trial's maximal sliding velocity (V_{max}), $[Ca^{2+}]$ that elicited half of the maximal velocity (pCa_{50}), and the steepness of the slope of the curve (Hillslope, *n*), which represents the cooperativity of the myosin heads (a steeper slope indicates a higher degree of cooperativity, Table 4.1). A scatterplot of the average velocities vs. pCa values demonstrated a reduction in V_{max} for RTFs from all Tm variants (Figure 4.1).

Conditions		Velocity Fit Parameters		
Tm	*pH*	*Vmax*	pCa_{50}	*n*
eWT	7.4	3.97 ± 0.15	6.83 ± 0.08	1.27 ± 0.30
eWT	6.8	2.23 ± 0.13*	6.67 ± 0.14	1.10 ± 0.33
H153A	7.4	3.81 ± 0.13	7.12 ± 0.10	2.07 ± 1.28
H153A	6.8	2.12 ± 0.12*	6.98 ± 0.14	1.11 ± 0.43
H276A	7.4	3.38 ± 0.14	6.80 ± 0.08	1.88 ± 0.49
H276A	6.8	2.34 ± 0.09*	6.55 ± 0.11	1.41 ± 0.32
DBL	7.4	3.56 ± 0.25	6.72 ± 0.13	1.65 ± 0.66
DBL	6.8	1.93 ± 0.10*	6.42 ± 0.12	1.21 ± 0.31

Table 4.1: Hill equation parameters generated from the fit of the Hill equation to velocity-pCa plots. V_{max} is a measure of maximal sliding velocity, pCa_{50} a measure of Ca^{2+}-sensitivity, and *n* indicates cooperativity (higher value indicates increased cooperativity). Values displayed are means ± SEM. *Indicates significant difference ($p<0.05$) vs. each Tm's 7.4 control value.

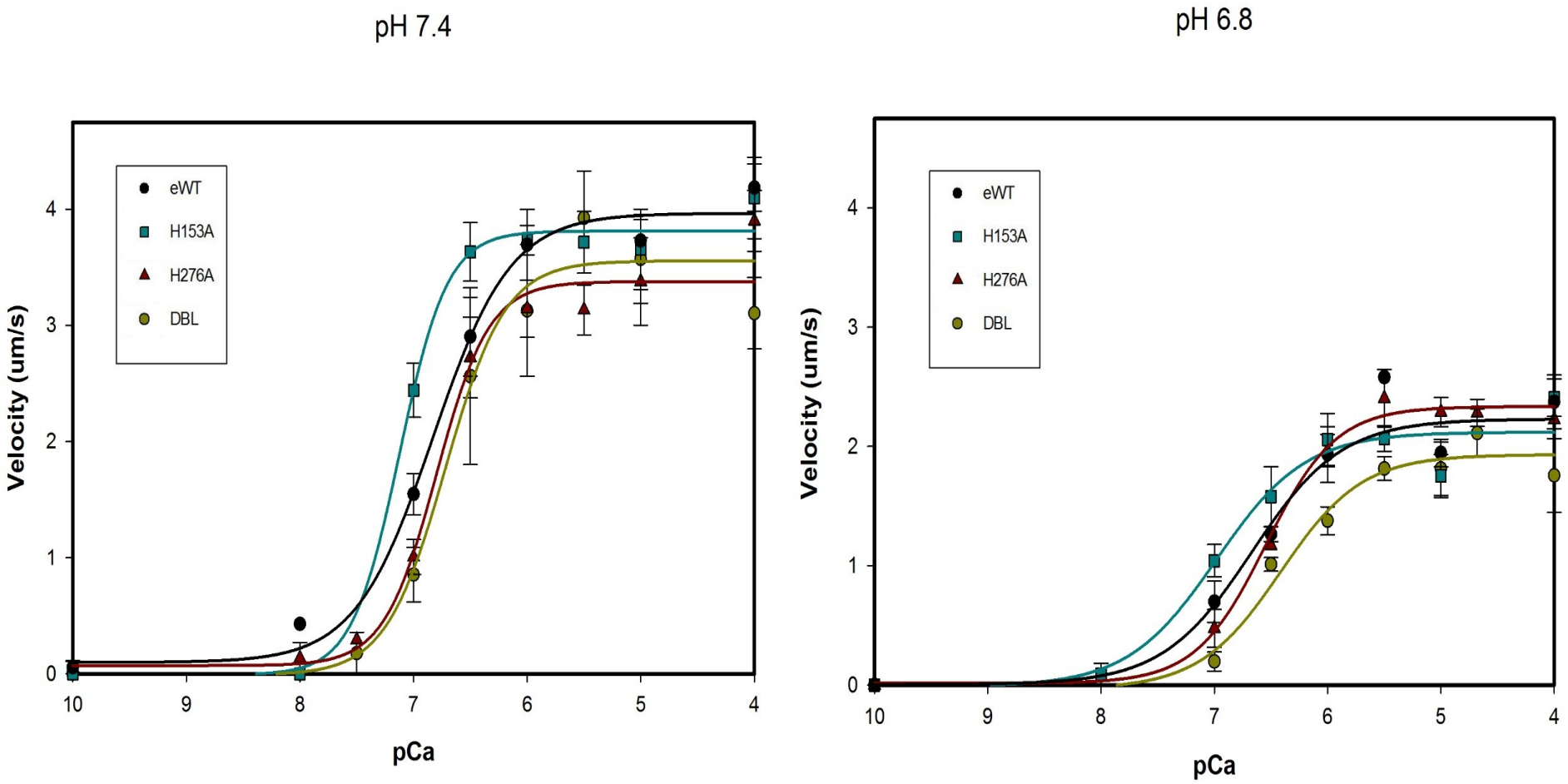

Figure 4.1: Velocity-pCa scatterplot graphs fit with the Hill equation. Scatterplot points represents mean velocity and bars represent SEM. Lines represent the fit from the Hill equation (see description in Methods).

4.1.1 – RTF maximal sliding velocity

The average V_{max} value for each of the four Tm variants at both pH levels was calculated by taking the average of all V_{max} values generated by the fit of the Hill equation to each experimental trial (Figure 4.2). As expected, lowering the pH from 7.4 to 6.8 resulted in a 43% average drop in the maximal sliding velocity of all the RTFs. This decrease is similar in direction and magnitude to previous findings for WT Tm (13, 68, 69). The drop in pH elicited significantly slower maximal sliding velocities for each variant of Tm used, with a 44% decrease for eWT, 46% for H153A, 36% for H276A, and 46% for H153A/ H276A shown in Figure 4.2. A two-way (pH x Tm) repeated-measures ANOVA of the data indicated that all Tm variants experienced a significant decrease in velocity from pH 7.4 to 6.8 ($p < 0.001$), but the magnitude of the decrease was similar among all the variants of Tm based on a non-significant pH x Tm interaction term ($p = 0.569$).

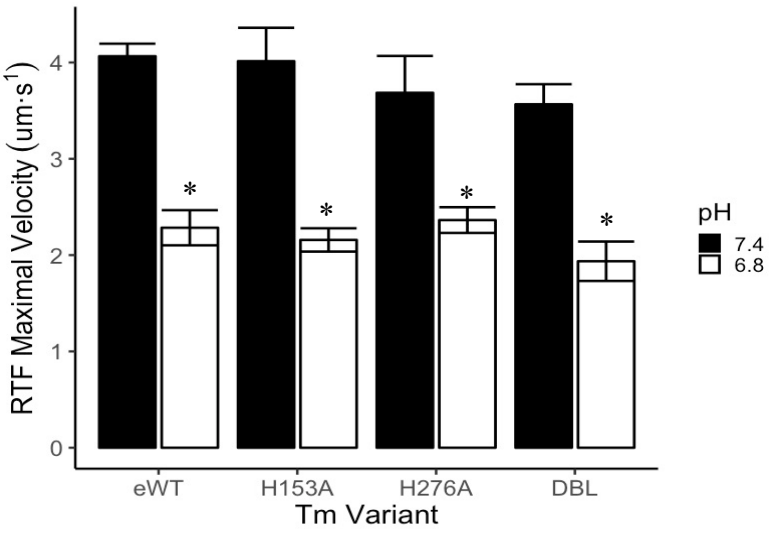

Figure 4.2: Bar graph of the mean V_{max} values calculated by averaging the V_{max} from each experimental trial. Bars are mean values ± SEM.
Indicates significant slower velocity vs each Tm's 7.4 control ($p<0.001$)

4.1.2- Relative change in maximal sliding velocity from pH 7.4 to 6.8.

The relative change in maximal sliding velocity from pH 7.4 to pH 6.8 was calculated by the equation:

$$(6.8\ V_{max} - 7.4\ V_{max}) / 7.4\ V_{max} * 100$$

The calculated relative change values were tested for significant differences using a one-way ANOVA. The results indicate decreases in velocity caused by lowering pH from 7.4 to 6.8 was similar across the different Tm variants ($p = 0.522$, Figure 4.3). The negative relative change values indicate the maximal sliding velocity of the RTFs were slower at pH 6.8 compared to 7.4 across all Tm variants.

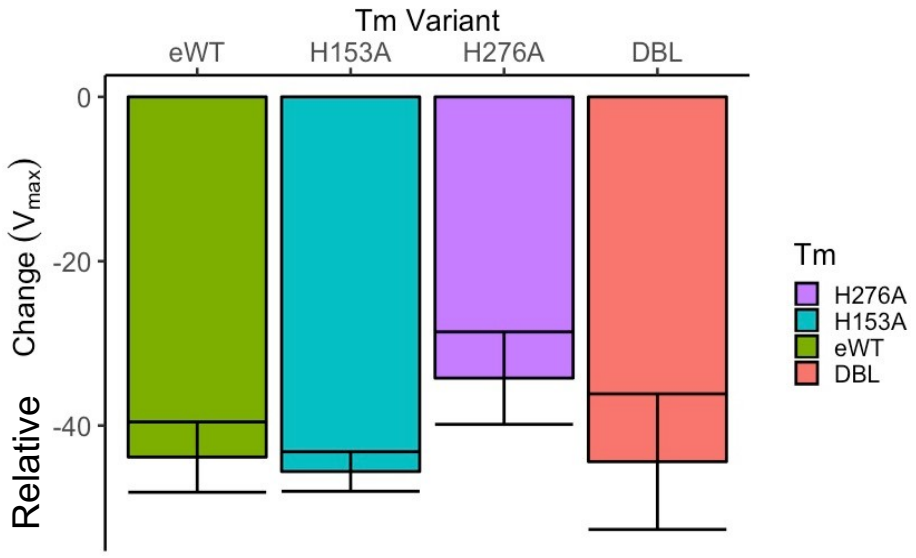

Figure 4.3: Percent change in the maximal sliding velocity of RTFs from pH 7.4 to 6.8. Negative values indicate the V_{max} at pH 6.8 was less than pH 7.4. Bars represent the mean value with SEM. No significant differences reported.

4.1.3 – pCa_{50} of velocity

The pCa_{50} parameter provides a measure of the calcium sensitivity of the RTFs. Higher pCa_{50} values correspond to higher calcium sensitivity and indicate that it required less free Ca^{2+} to activate the RTF to half of its V_{max}. A two-way repeated measures ANOVA indicated the pCa_{50} values were not significantly affected by acidosis ($p = 0.541$), and the differences did not depend on the variant of Tm (interaction term pH x Tm, $p = 0.781$, Figure 4.4). However, there was a significant main effect of Tm variant ($p = 0.039$) and a Tukey post-hoc test identified the double mutant as having a significantly lower pCa_{50} compared to the H153A single mutant at pH 7.4 but not pH 6.8 ($p = 0.042$). This result indicates that while the Ca^{2+}-sensitivity of all RTFs were unaffected by acidosis, the H153A/H276A double mutant required more Ca^{2+} to achieve half of its maximal velocity at pH 7.4 compared to the H153A single mutant.

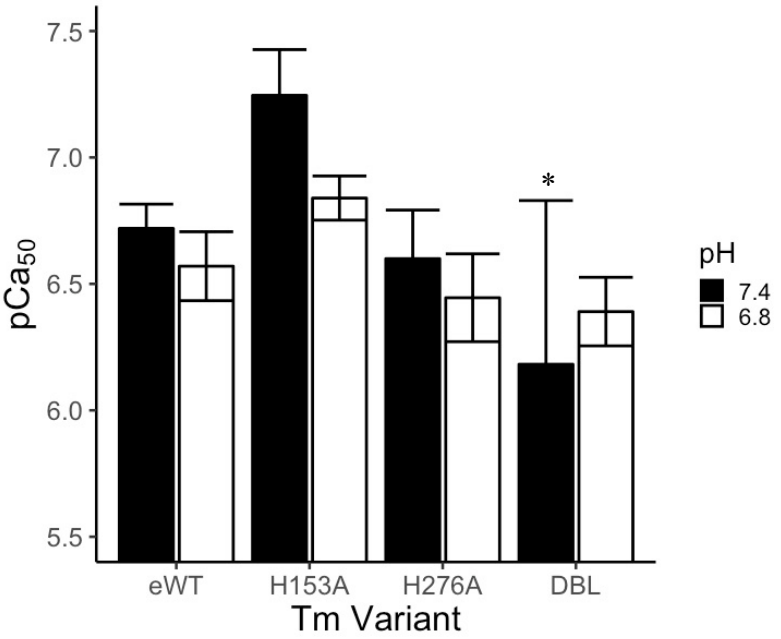

Figure 4.4: Bar graph of the average pCa_{50} calculated from the average of the pCa_{50} values from each experiment trial. Bars are mean values ± SEM. *Significant decrease relative to H153A at pH 7.4.

4.1.4 – Effects on hillslope coefficient (*n*)

There were no effects on the *n* of the velocity-pCa curves between the RTFs reconstituted with each of the four Tm variants. A two-way repeated measures ANOVA comparison indicated no significant differences between pH ($p > 0.05$), Tm ($p > 0.05$), or the interaction term ($p > 0.05$, Figure 4.5). This result suggests that the mutations or acidosis did not alter the cooperativity of myosin binding. The high variation in the data is due to inconsistencies in the fit of the Hill equation to each experimental trial.

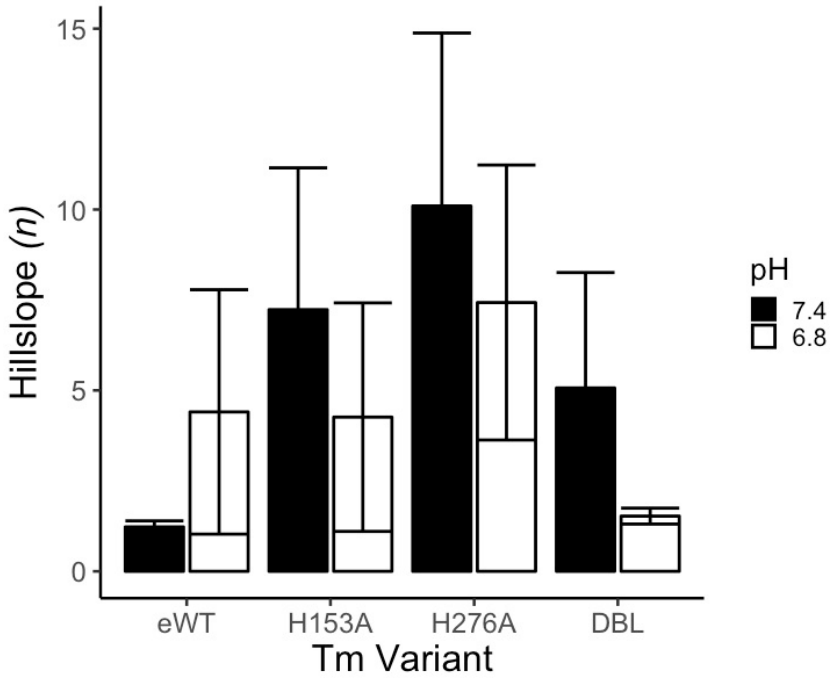

Figure 4.5: Bar graph of the average hillslope coefficient (*n*) values calculated from the average of *n* obtained from each experimental trial. Bars are mean values ± SEM. No significant differences reported.

4.2 – Percentage of Moving Filaments Data

Scatterplots of the percentage of filaments moving vs pCa were also fitted with the Hill equation. As a result, the Hill parameters were generated and used for comparison in statistical testing similarly to methods used for the velocity data analysis (Figure 4.6). The parameter values generated from the fit of the Hill equation to the percentage of moving filaments data are shown in Table 4.2.

Conditions		Percentage of RTFs Moving Hill Fit Parameters		
Tm	*pH*	*Percent Moving*	*pCa50*	*n*
eWT	7.4	84% ± 2%	6.95 ± 0.04	3.20 ± 1.45
eWT	6.8	78% ± 3%	6.75 ± 0.06	2.01 ± 0.33
H153A	7.4	82% ± 2%	7.15 ± 0.08	2.30 ± 1.14
H153A	6.8	78% ± 3%	6.96 ± 0.07	1.59 ± 0.45
H276A	7.4	82% ± 5%	6.80 ± 0.10	1.64 ± 0.53
H276A	6.8	77% ± 2%	6.58 ± 0.07	1.82 ± 0.41
DBL	7.4	82% ± 1%	6.85 ± 0.03	3.43 ± 0.56
DBL	6.8	69% ± 7%	6.25 ± 0.24#	1.08 ± 0.56

Table 4.2: Hill equation parameters generated from the fit of the Hill equation to percentage of moving filaments-pCa plots. Mean values ± SEM. # Indicates significant interaction of pH and Tm ($p<0.05$). Values shown were generated from the Hill equation fit in Figure 4.6.

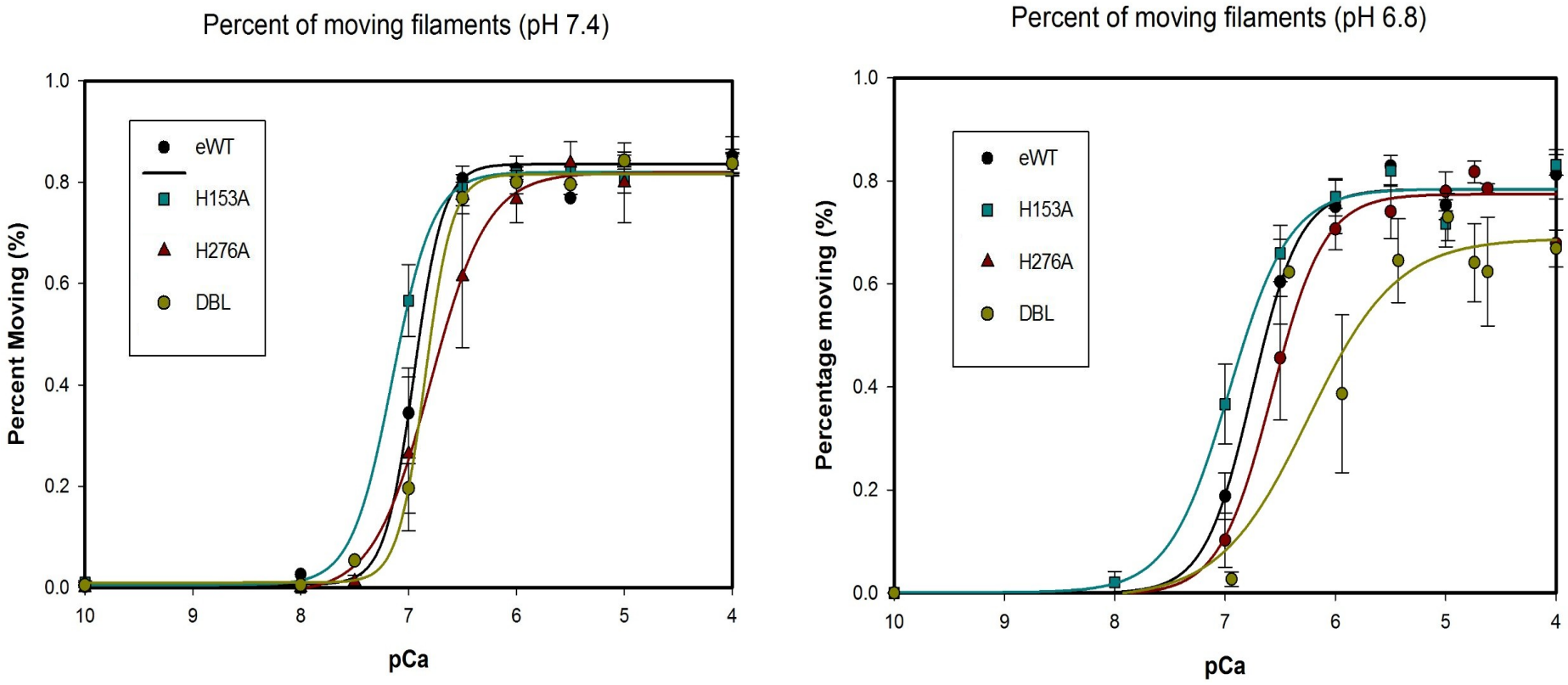

Figure 4.6: Percentage of moving-pCa scatterplot graphs fitted with the Hill equation. Scatterplot points represent mean velocity and bars show SEM. Lines represent the fit from the Hill equation (see description in Methods).

4.2.1 – The effects of pH and tropomyosin on the percentage of moving filaments

The results of a two-way repeated measures ANOVA indicated no significant differences in the maximal percentage of moving filaments (Tm variant $p = 0.16$, pH $p = 0.058$, Tm x pH, $p = 0.773$). This measurement shows that pH affects the maximal sliding velocity of the RTFs without changing the percentage of moving filaments.

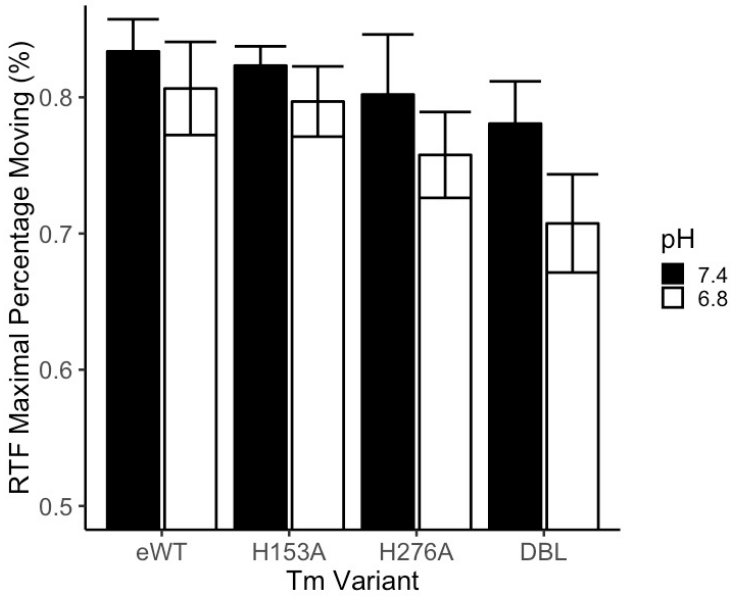

Figure 4.7: Average percentage of moving filaments. Bars are mean values ± SEM. No significant differences.

4.2.2 – pCa_{50} of the percent of moving filaments

A two-way repeated measures ANOVA indicated a significant interaction (Tm x pH, $p = 0.025$) in the pCa_{50} of the percent moving data. A Tukey post-hoc analysis identified that the H153A/H276A double mutant had a significantly lower pCa_{50} at pH 6.8 compared to the other three Tm variants (Figure 4.8). The pCa_{50} of percentage moving indicates that the H153A/H276A double mutant required a higher concentration of Ca^{2+} to achieve half of the maximal number of filaments moving. Additionally, both the eWT and H153A/H276A double mutant had significantly lower pCa_{50} values at pH 6.8 compared to their respective pH 7.4 control. These results suggest that the double mutant may be more susceptible to acidosis (i.e. decrease in pH) than the other three Tms.

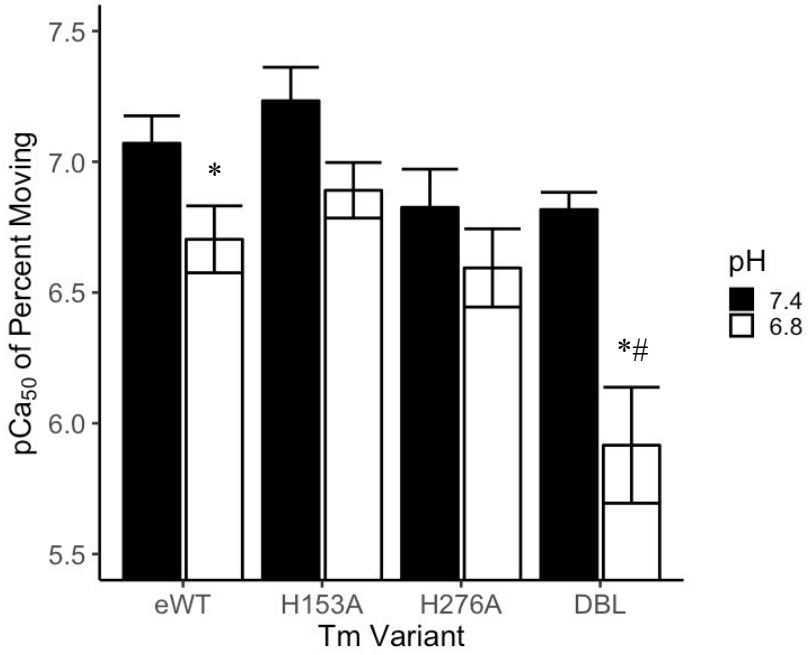

Figure 4.8: pCa_{50} of the percentage of moving filaments. This measurement represents the Ca^{2+} concentration required to get half the filaments moving. Bars are mean values ± SEM. *Significant difference vs 7.4 control. #Significant difference vs all other Tm at pH 6.8.

4.2.3 – Relative change in pCa50 of the percent moving

A calculation of the relative change in the pCa_{50} values between pH 7.4 and 6.8 for the percentage moving data was made using the following formula:

% change = (6.8 pCa_{50} – 7.4 pCa_{50})/7.4 pCa_{50} * 100

These calculated relative change values were analyzed in a one-way ANOVA which identified a significant difference in relative change of the pCa_{50} of the percentage of moving filaments data ($p<0.05$). A Tukey post-hoc test indicated that the H153A/H276A had a greater decrease in the pCa_{50} compared to both the H153A and H276A single mutants ($p<0.05$) suggesting the double mutant Tm was more affected by the drop in pH than either of the single Tm mutants.

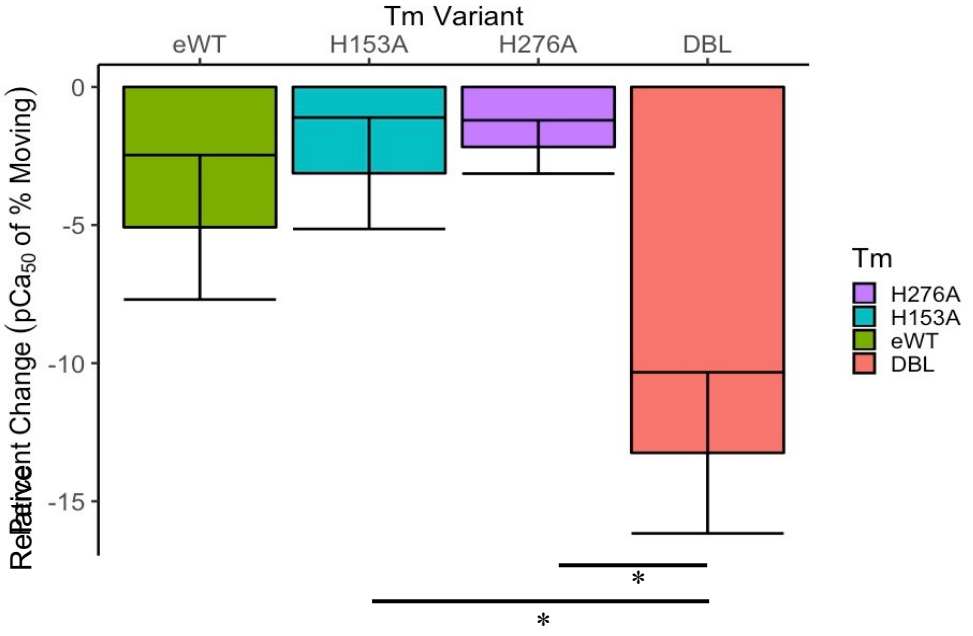

Figure 4.9: Relative change in pCa_{50} from the percentage of moving filaments data. Negative values indicate the pCa50 at pH 6.8 was less than pH 7.4. Bars are mean values ± SEM.. *Indicate significant differences from Tukey multiple comparisons of means test*

4.2.4 – Hillslope coefficient of percentage moving

Lastly, the *n* values from the percentage moving data were compared using a two-way repeated measures ANOVA and the results indicated no significant effects of pH ($p = 0.695$), Tm ($p = 0.45$), or interaction (pH x Tm, $p = 0.52$, Figure 4.10). Therefore, a similar cooperativity of myosin binding under all conditions was observed. The high variation in the data is due to inconsistencies in the fit of the Hill equation to each experimental trial.

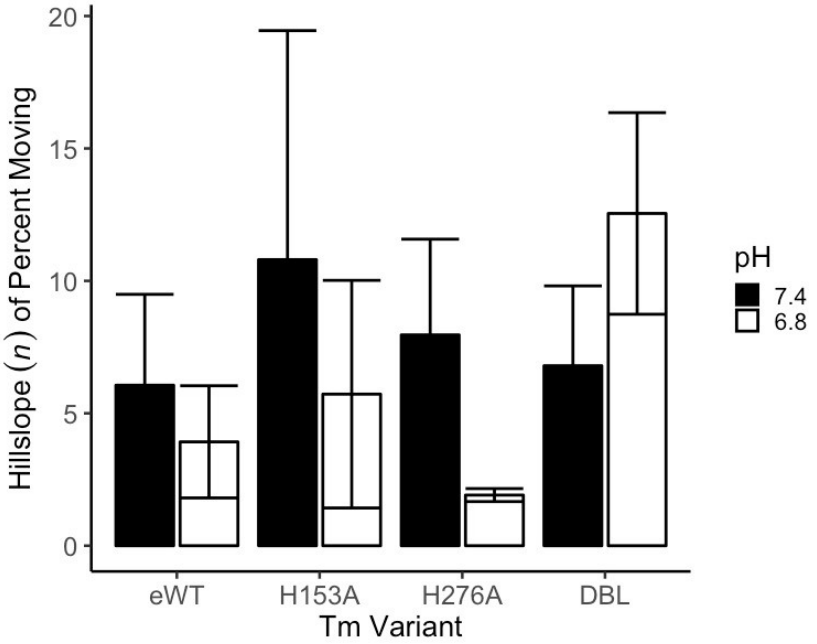

Figure 4.10: Average hillslope coefficient from the percentage of moving filaments data. Bars are mean values ± SEM. No significant differences reported.

CHAPTER 5

DISCUSSION

Tropomyosin has previously been implicated to be an important modulator of the pH-dependence of active tension in muscle fibers (20). This observation helped motivate the present study with the purpose to elucidate the mechanism underlying this effect. To address this, two His residues in Tm's structure were identified as potential targets because of their physiological relevant side chain pKa of ~6.5. By replacing one or both His residues in the Tm structure we were able to test whether an acidosis-induced charge change of His residues or the location of the amino acids were depicting the Tm response. We hypothesized that this would alter function under acidic conditions and that it may be more pronounced based on the location of the mutation. However, our current findings suggest that there are no effects of His charge change or location on the V_{max}, pCa50, and hillslope parameters of velocity. Additionally, the His charge and location had no effects on the maximal percentage of moving filaments or the hillslope of the percent moving data. The only significant result occurred in the pCa_{50} of the percentage moving data (pH x Tm interaction). A Tukey post-hoc test identified that the double mutant had a significantly lower pCa_{50} of the percentage moving data at pH 6.8 indicating more Ca^{2+} was required to get half of the filaments moving during acidosis compared to the other three Tm variants. However, due to the majority of non-significance results in five of the six parameters tested, it is possible that there was a type-1 error falsely reporting a significant result. Overall, the results from this study provide evidence that Tm's His residues play no role in mediating the pH-dependent effects of acidosis on muscle velocity.

5.1 – pH affects the maximal sliding velocity of RTFs equally across the Tm variants

The results from the statistical analyses indicate that the differences in the maximal sliding velocities of RTFs are **not** dependent on the number of His residues present in Tm, the charge, or their location. We saw dramatic differences in the maximal sliding velocity of all RTFs as a result of decreasing the pH from 7.4 to 6.8. However, this large drop in maximal sliding velocity in response to acidosis was expected and prior observations show the unloaded shortening velocity (a measure similar to V_{max} (72)) of muscle fibers is reduced by up to 25% in cardiac muscle fibers (pH 6.6), 25% in type I fibers (pH 6.2), and 32% in type II fibers (pH 6.2) from control conditions (37, 64). Additionally, decreases in the maximal sliding velocity of actin filaments in previous IVM assays show a 25-50% reduction in the filament sliding speed when the pH of the final motility buffer is lowered (11, 13, 26). Our data is consistent with these previously reported effects of acidosis on muscle velocity as we observed an average 43% decrease in the V_{max} of the RTFs at pH 6.8 relative to pH 7.4. This large decrease in velocity has largely been attributed to a direct effect of acidosis on myosin as acidosis is believed to slow the rate of ADP release (11). The effects on myosin are also thought to be the main contributor to the acidosis-induced depression in maximal velocity as there are comparable changes in the relative decrease in velocity that occur as a result of acidosis with both regulated and unregulated RTFs in IVM (11, 13, 26). Together, these results suggest that the removal of one or both His residues from Tm, and by association the charge change potential, has little or no effect on the maximal sliding of RTFs in an unloaded in vitro motility assay. Therefore, this suggests that the majority of the decrease in velocity is due to the depressive effects of acidosis on myosin function.

5.2 – His residues in Tm and pH have no effect on the pCa_{50} or Hill coefficient

We originally hypothesized that His residues would attenuate the pCa_{50} of the maximal sliding velocity. However, the pCa_{50} of the velocity was unaffected by acidosis in this study. While this has been observed before (13), in the context of IVM with our Tm variants an unchanged pCa_{50} indicates that His residues do not have any effects on the acidosis-induced depression in Ca^{2+}-sensitivity of muscle velocity. Furthermore, this shows that unloaded velocity measurements at pH 6.8 are not the best indicator of the severe effects that acidosis can have on the Ca^{2+} sensitivity of the thin filament. While significant effects of acidosis on the Ca^{2+}-sensitivity of RTFs have been reported before in IVM at pH 6.8 (64), the data were collected at a lower temperature (25°C) than the present data (30°C). Moreover, lowering temperature was shown to decrease Ca^{2+}-sensitivity in the same study (68). The unchanged pCa_{50} of velocity-pCa is in stark contrast to the large decrease in Ca^{2+}-sensitivity that acidosis has on the force-pCa relationship measured in muscle fibers, Figure 1.1 (17) and is most likely the result of the combined effects of several factors. First, an increase in tension has been observed in muscle fibers incorporated with NEM-S1 myosin when compared to control fibers (20). This indicates that an increase in strongly bound myosin heads increases thin filament activation. Furthermore, it has been suggested that acidosis prolongs myosin's attachment lifetime under acidic conditions (11). This would increase thin filament activation during acidosis resulting from an increase in strongly bound myosin heads due to the increase in t_{on}. However, instead of an increased Ca^{2+}-sensitivity, we observed no change in the pCa_{50} of RTF velocity showing that acidosis is a complicated and multi-faceted issue. The current data suggests that the increase in thin-filament activation from the H^+

induced prolongation of myosin attachment lifetime counteracts the depressive effects of acidosis on thin filament Ca^{2+}-sensitivity (Figure 5.1) that results in an unchanged pCa_{50} of velocity-pCa.

5.3 – No effects of Tm or pH on the maximal percentage of moving filaments

There were no significant decreases in the maximal number of moving filaments caused by either the Tm variant or pH in this study (see Figure 4.7). These results differ from what was previously reported from our lab as Debold et al. 2012 showed a significant decrease in their percentage of RTFs moving in IVM as a consequence of lowering the pH to 6.8 from 7.4. However, those experiments included an additional pH factor level (6.5). Consequently, this increased their sample size and increased their statistical power to detect the small change in the percentage of moving filaments that results from changing pH from 7.4 to 6.8. Overall, the percentage of moving filaments data calculated for our Tm variants indicates that acidosis did not significantly affect the maximal activation of the RTFs, even though acidosis had prominent effects on the maximal sliding velocity. This suggests that acidosis slows all the RTFs equally (see Figure 4.1). This notion is further supported by examining a histogram of individual filament velocities at both pH 7.4 vs. 6.8 (Figure 5.2).

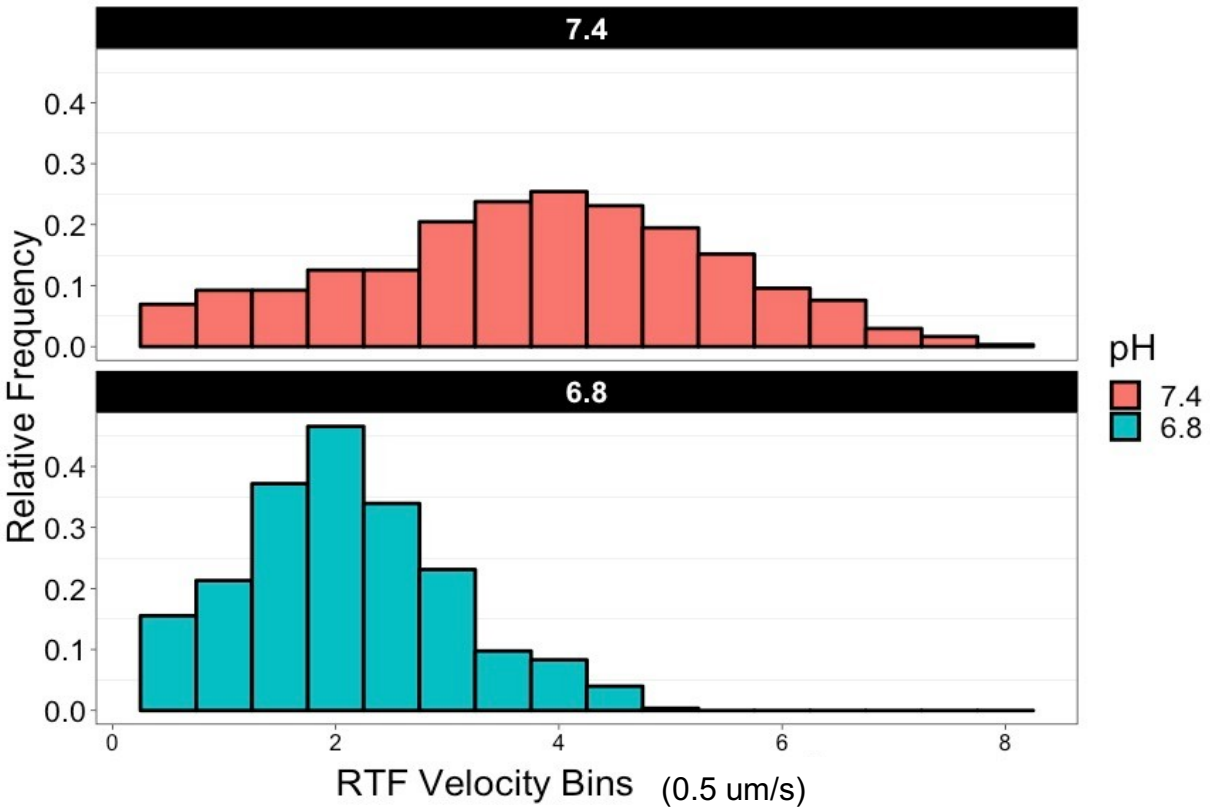

Figure 5.1: Histogram of individual filament velocities at both pH 7.4 (red) and 6.8 (blue). Each bar represents a 0.5 um/s range relative frequency bin. Data collected on RTFs with eWT Tm at pCa 4.

Acidosis caused a leftward shift in the distribution of the relative frequency of filament velocity histogram. As a result, this accounts for the overall slower average velocity without increasing the relative frequency of slow or non-moving filaments and provides an explanation for the preserved percentage of moving filaments value (see Figure 4.6).

Therefore, the acidosis-induced depression in velocity is not likely to be mediated or involve protonation of the His residues. Indeed, maybe Tm is not involved in these effects at all since the magnitude of the depression in RTF velocity observed during acidosis in our experiments is similar to what has been observed with unregulated actin filaments (11, 13). This suggests that the depressive effects that acidosis has on muscle velocity results primarily from effects on myosin.

5.4 – Possible explanations for the non-significant effects of the Tm mutations

The results of this study suggest that the His residues present in Tm do not mediate or modulate the depressive effect of pH effects on muscle velocity observed during exercise-induced acidosis, contradictory to my original hypothesis which was that histidine residues mitigate the depressive effects of acidosis. This hypothesis was proposed based on the assumption that Tm's position on actin is dictated by sparse and weak electrostatic interactions (27) when not constrained by Tn in the "blocked-state". This was coupled with reports that acidosis increased the temperature required to dissociate Tm from actin (71), and was interpreted as acidosis stabilizing Tm in the "blocked-state". However, the results suggest that this is not the case, at least for velocity under the conditions we tested. There are several potential reasons why these data were not consistent with the hypothesis.

5.4.1 – Histidine residues do not interact with actin in the "blocked-state"

Figure 2.11 (pg. 21) depicts a model to explain the original hypothesis. The schematic was drawn to be consistent with known Tm/actin interactions (45) and based upon tropomyosin spanning the distance of seven actin monomers and periodically interacting with actin via small clusters of positively charged amino acid residues on the actin surface. My hypothesis was that sparse and weak electrostatic interactions occur between the negatively charged surface of Tm with the positively charged residues on actin, and therefore that a His charge change, as would occur when the pH was decreased, could affect the Tm/actin interaction and result in a change in its relative position within its dynamic equilibrium. While originally it appeared that the position of H153 and H276 were near known actin binding sites, Glu-142 and Glu-263 (45) it seemed plausible for

His charge change to affect these interactions by adding a nearby positive charge that would destabilize the "blocked-state" allowing Tm to more readily shift between its "blocked-state" to "closed-state" upon Ca^{2+} binding Tn mitigating some of the depressive effects of acidosis, but this does not seem to have been the case.

The structure and organization of Tm's primary structure was detailed in Figure 2.4 (pg. 9). Despite the close positional proximity to known actin binding sites, both His residues lie within the β-zone of its pseudo-repeat. Only the amino acids in the α-bands are believed to make contact with actin in the "blocked-state", while the β-band residues are thought to make contact in the "closed-state" and "open-state" (28, 50, 64). Since the two His residues are in the β-band of their respective pseudo-repeats they are **not** thought to make contact with the surface of actin in the "blocked-state" indicating that their charge change could not destabilize the "blocked-state" as originally hypothesized. Further information detailing known actin binding sites in both the α- and β- bands is shown in Figure 5.3.

Figure 5.2: Primary sequence of Tm organized into seven pseudo-repeats divided into α- & β- bands. Red arrows indicate known actin binding sites From Redwood & Robinson 2013.

The division of each pseudo-repeat into α- & β- bands is more important than originally thought. A more accurate hypothesis of the Tm/actin interaction including the division of the α- and β-bands of the pseudo-repeats suggests that His charge change would not affect the Tm/actin interaction in the blocked state (Figure 5.4). Therefore, it is possible no changes were observed in the Hill equation parameters because the location of His residues prevented the charge from affecting Tm/actin interaction.

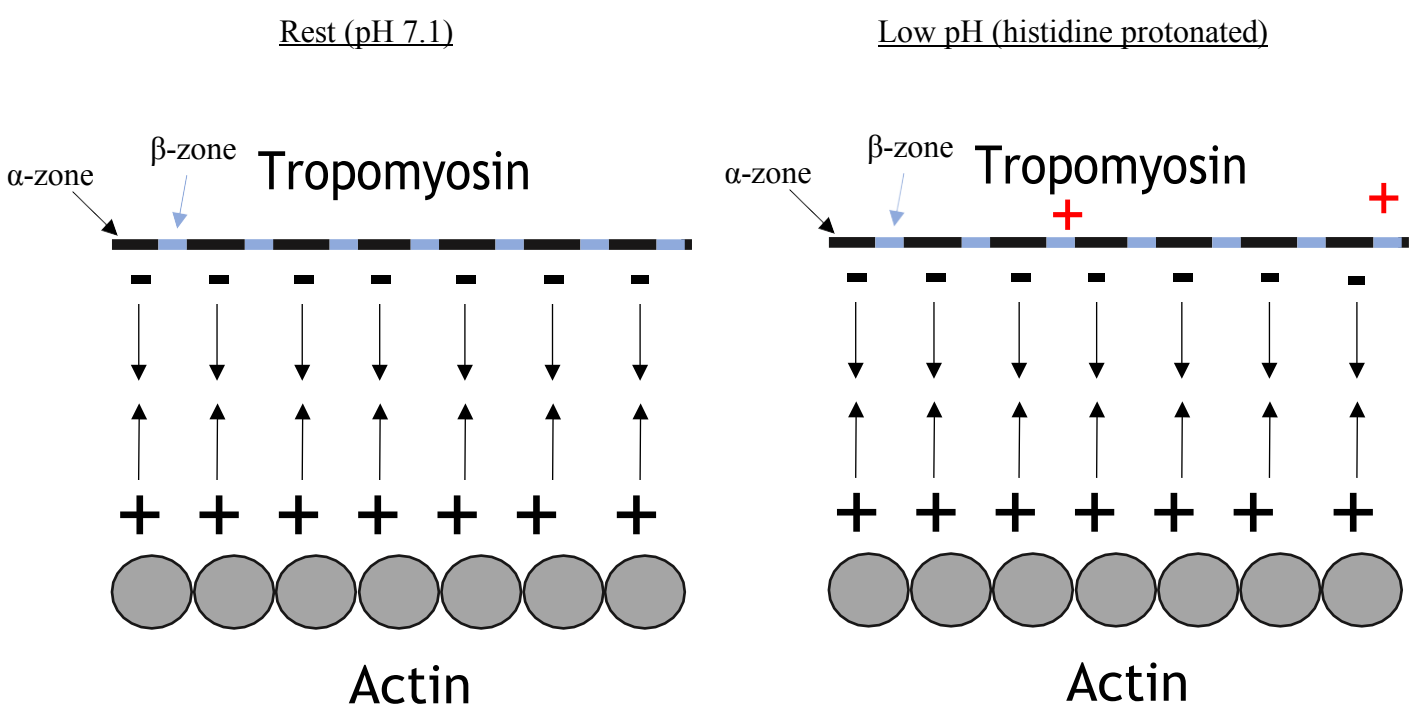

Figure 5.3: Updated cartoon model of how histidine residues do **NOT** make contact with actin. Histidine protonation still occurs but most likely would not have any intermolecular effects.

5.4.2 – pH 6.8 did not cause the majority of His residues to protonate dampening the full effect of His charge change

While the location of histidine residues in the β- bands may prevent them from interacting with actin in the "blocked-state", another alternative explanation for the non-significant results is that pH 6.8 did not elicit the majority of His residues to change charge which limited the extent of any observable effects of the charge change. It was previously discussed that the His location prevents it from affecting the intermolecular contacts Tm makes with actin, but the effects of His charge change could still change intramolecular interactions within the Tm molecule which are important determinants of

Tm's shape, flexibility, and head-to-tail stability (44, 62). H276 lies in the head-to-tail overlap region within an amino acid sequence that contributes to Tm's overall stability by imparting a rigidity between each Tm molecule allowing the whole Tm polymer to translocate upon myosin binding providing myosin cooperativity, and H153 lies in a less stable amino acid sequence that contributes to Tm's flexibility which determines Tm's ability to allosterically regulate myosin cooperativity (54, 62). Since Tm's "e-g" pairs and head-to-tail overlap involve ionic interactions (23,39), changes in His charge could have effects on those interactions that were undetectable at the pH we experimented with.

The IVM assays were performed at pH levels that simulated rest (pH 7.4) and moderate levels of fatigue (pH 6.8), but pH 6.8 is above the pKa of the His side chain. A pH greater than the His side chain pKa indicates that the majority of the His residues are deprotonated. The Henderson-Hasselbach equation can be used to estimate the fraction of His residues that are protonated at each pH level used in this experiment:

1) $pH = pKa + \log_{10}([A^-]/[HA])$

2) $\log_{10}([A^-]/[HA]) = pH - pKa$

3) $[A^-]/[HA] = 10^{pH - pKa}$

pH 7.4: $10^{7.4 - 6.5} = 7.94$

By taking the reciprocal of the solution from the pH 7.4 Henderson-Hasselbach calculation above, the ratio of protonated to deprotonated His residues is estimated to be about 1:8. This proportion indicates that 11% of His residues would be protonated at pH 7.4. These calculations can also be made for pH 6.8:

pH 6.8: $10^{6.8 - 6.5} = 2.00$

By taking the reciprocal of the solution from the pH 6.8 calculation above, the ratio of protonated to deprotonated His residues is estimated to be about 1:2. This proportion indicates that 33% of His residues would be protonated at pH 6.8. By changing the pH from 7.4 to 6.8, the percentage of protonated His residues increased from 11% to 33%. This small change in the percentage of protonated His residues may have limited our ability to detect differences in function resulting from effects of His charge change.

While our results show that pH 6.8 did not elicit a large change in His protonation it was chosen because it causes a large decrease in $V_{max,}$ as shown by our ~43% reduction in unloading sliding velocity observed in the present experiments. Seemingly, by decreasing the pH to levels below the His side chain pKa of 6.5 we could increase the percentage of protonated His residues providing better resolution for the effects of His charge change on RTF velocity.

pH 6.2: $10^{6.2-6.5}= 0.5$

By taking the reciprocal of the solution from the pH 6.2 calculation above, the ratio of protonated to deprotonated His residues is estimated to be about 2:1. This proportion indicates that a majority 66% of His residues would be protonated at pH 6.2. A larger number of His residues that are protonated should correspond to more pronounced effects of His charge change on the Hill equation parameters. However, previous results show that IVM conducted at pH 6.5 have too large of a depressive effect on RTF sliding velocity and only extremely slow motility can be observed at saturating Ca^{2+} levels (12). This results in unreliable estimates of the pCa_{50} and *n* as the velocity-pCa curves lose their defining sigmoidal curve as shown in Figure 5.5. As for the current data, an explanation for our non-significant results is that pH 6.8 did not cause a large

enough increase in the percentage of protonated His residues that prevented the full effect of His charge change to be observed by our measurements.

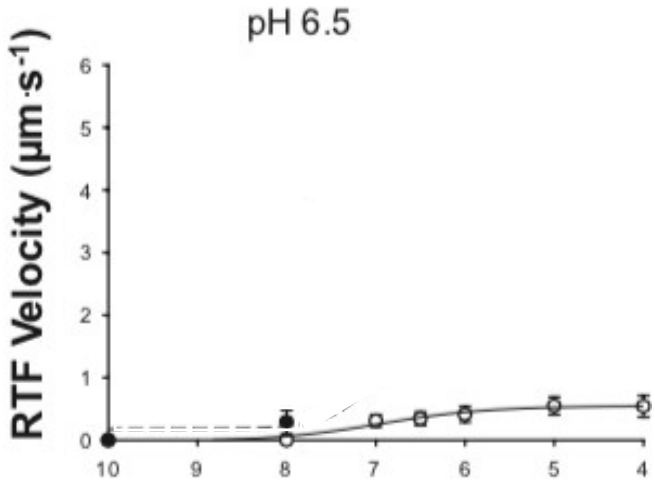

Figure 5.4: In vitro motility at pH 6.5. Almost all motility is stopped except for saturating Ca^{2+} levels. Adapted from Debold et al. 2012.

5.4.3 –V_{max} is independent of Tm under the detachment limitations of IVM

For this project, we measured unloaded sliding velocity of our RTFs and not the force generating capacity. IVM is similar to the unloaded shortening velocity measurement used in muscle fiber experiments, and as a result, we were studying the effects of His protonation at one extreme of the force/velocity and load/power relationships (Figure 5.6).

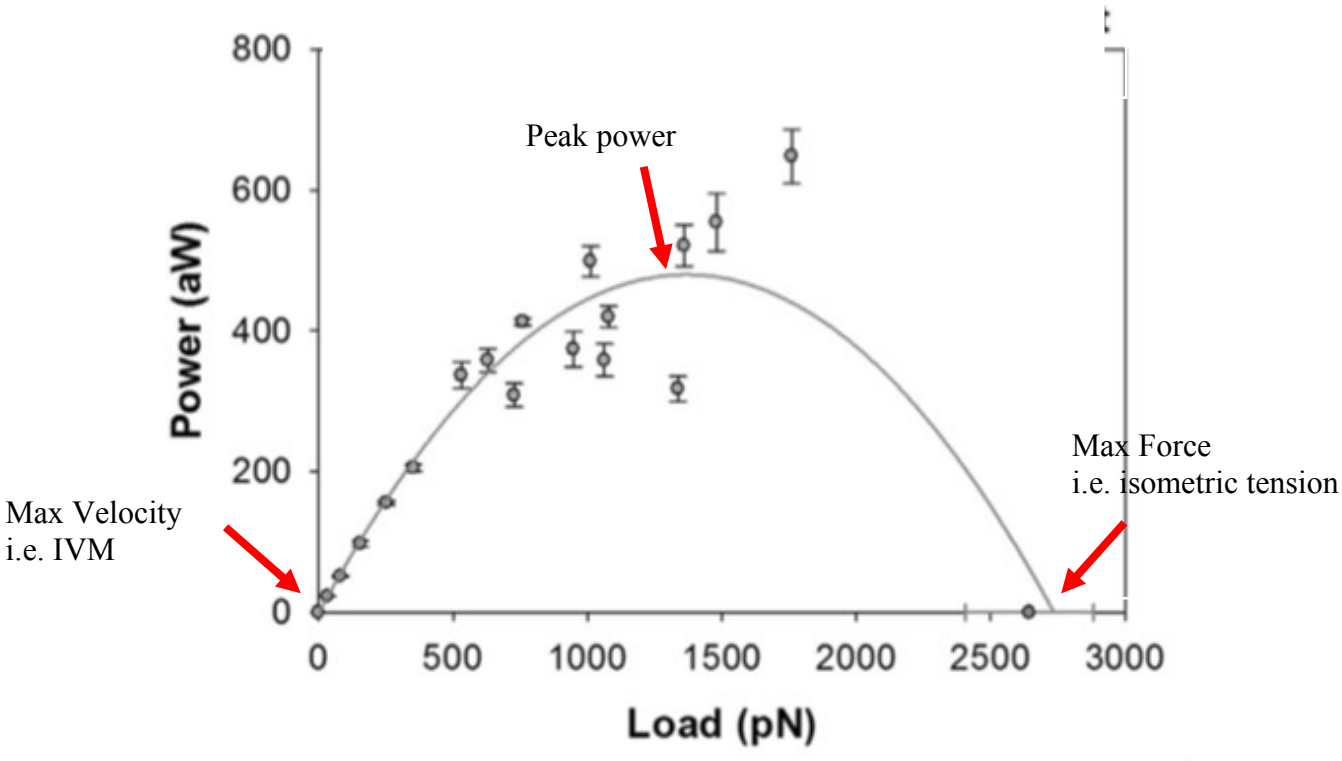

Figure 5.5: IVM is at the left extreme of the load-power curve. Consequently, we studied the effects of His protonation in determining unloaded velocity. Adapted from Karabina et al. 2015.

In the IVM for this study, the myosin that were fixed to the glass coverslips were producing a negligible amount of force. Any load would result as a combination of the mass of the actin filaments and the viscous drag imposed on the filaments as they glide through the motility buffer. As a result, we sampled the effect of His protonation under unloaded conditions and concluded that the number of His residues, their location, and their charge have no effect on muscle velocity at either pH 7.4 or 6.8. It is possible the detachment limitation of IVM limited the ability for us to observe changes in Tm function. The following equation defines the molecular determinants of IVM max velocity (V_{max}) (32, 33).

Velocity = d/t_{on} (detachment limited)

Velocity is dependent on the distance that the myosin lever arm rotation can displace the actin filament and is inversely proportional to the myosin attachment lifetime (t_{on}). Higher velocities can be achieved by increasing the displacement of each lever arm rotation or by decreasing t_{on}. Moreover, most changes in velocity as a result of acidosis are solely dependent on changes in t_{on} as the distance of lever arm rotation is conserved to ~10nm during productive events at low pH (11) indicating that myosin detachment is the main determinant of IVM velocity.

In IVM, the successive binding of myosin heads is necessary to continually propel the RTFs at maximal velocity. In fact with regulated RTFs, once sufficient Ca^{2+} levels are reached to ensure multiple heads are bound to the RTFs allowing for continual movement velocity becomes independent of $[Ca^{2+}]$ (29). Examination of histograms of the relative frequency of RTF velocity across a range of pCa values indicates pCa 6 as the critical $[Ca^{2+}]$ threshold needed to allow for continual movement of most RTFs through solution (Figure 5.7).

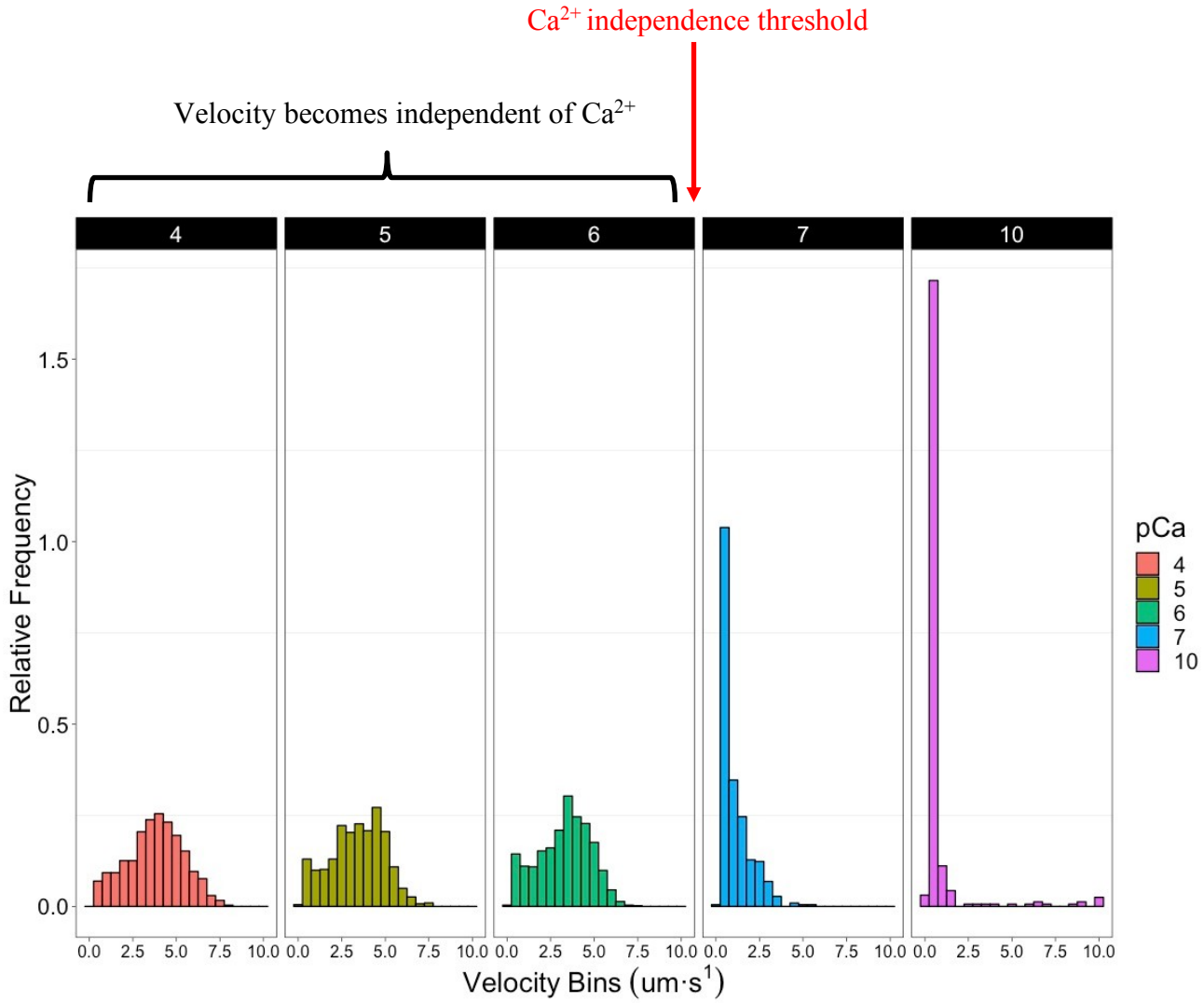

Figure 5.6: Histogram of individual filament velocities separated by pCa value. Each bar represents a 0.5 um/s bin. Data collected on RTFs with eWT Tm.

Once sufficient Ca^{2+} levels are obtained (pCa 6) that allows for multiple myosin heads to be attached and continually move RTFs, the role of Ca^{2+} in determining velocity and V_{max} is diminished leaving myosin detachment as the largest determinant of velocity. Indeed, the regulatory proteins have been shown to increase the sliding speed of actin filaments in IVM compared to naked actin alone, but this effect has largely been attributed to the presence of Tn with Tm showing no effect on cross-bridge cycling at high myosin surface densities as was used in the present experiments (29, 73).

Considering Tm function is dependent upon Ca^{2+} binding Tn, if V_{max} is independent of Ca^{2+}, then it must also be independent of Tm, or in our case Tm variant. This is further evidenced by the similar relative drop in IVM velocity during acidosis exhibited in both unregulated and regulated actin filaments (10, 12) indicating that while the regulatory proteins increase velocity acidosis is mostly affecting the myosin. As a result, the detachment limitations of muscle velocity could explain the results of our Tm mutations having no effect on the maximal sliding velocity of our RTFs.

5.5 – Conclusion

Despite our non-significant results, the current data is informative in understanding the mechanisms underlying the depressive effects of acidosis and leaves new avenues of research to explore. While we provided an answer to the proposed research question with these experiments showing His protonation has no role in mediating the pH-dependent effects of mild acidosis (pH 6.8) on muscle velocity. It is unknown how extreme levels of acidosis (< pH 6.5) might affect Tm function through imparting larger changes in His protonation. Additionally, the current data cannot further explain the Tm based pH dependence of active tension in muscle fibers as originally observed by Fujita & Ishiwata (1999). Tm may not play a role in mediating the pH dependence of muscle velocity, but it remains unknown whether or not His protonation is the underlying mechanism that determines Tm's ability to mediate the pH-dependent behavior of myosin force-generating capacity and the Ca^{2+}-sensitivity of force.

5.6 - Potential Future Directions to Test Alternative Hypotheses

5.6.1 - Do the Tm mutations affect the Ca^{2+}-sensitivity of force?

A future direction is to test the hypothesis that His protonation mediates the pH dependence of active force production providing a mechanism underlying the effect originally observed by Fujita & Ishiwata (1999). The addition of α-actinin, an actin binding protein that forms the z-discs in the muscle's sarcomeres, to the IVM assay imposes a frictional load that the myosin must work against in order to move RTFs (24). As a result, active force production and power output can be measured in IVM under both normal and fatiguing pH levels (24, 35). Higher α-actinin concentrations are representative of a higher load in the IVM and require myosin to produce more force to move the RTFs relative to lower concentrations. As a result, the velocity measures of the RTFs in this loaded IVM would require some of the attachment limited considerations that determine the development of force. It is possible the effects of His protonation are conserved to active force production since force is attachment limited instead of being detachment limited like velocity (22):

Force = # of attached XBs * force per XB (attachment limited)

Force production is proportional to the number of attached cross-bridges and the force produced by each individual attached cross-bridge. Higher force output can be achieved by either increasing the number of strongly bound heads, increasing the force per cross-bridge, or a combination of both these factors. The role of Ca^{2+} in thin filament activation is to increase the number of attached cross-bridges (30). Since Ca^{2+} effects are in part mediated through Tm's position on actin, testing our Tm mutants under the attachment limitations of force production may produce different results of His location and charge

change on Tm function during acidosis since the force-pCa and velocity-pCa relationships are determined by different limiting factors (13, 30).

5.6.2 - Would a lower pH elicit a Tm-mediated effect on velocity?

We are interested in measuring the effects of acidosis on Tm, but the debilitating effects of acidosis on myosin's ability to propel RTFs in IVM is a major limiter in our present attempts to explore the role of Tm in acidosis (see Figure 5.5). Henderson-Hasselbach calculations show that pH 6.2 would elicit 66% of His residues to change charge and would provide more pronounced and detectable effects. Seemingly, if we could alleviate some of the depressive effects of acidosis off of the myosin by increasing RTF sliding velocity and restore the defining sigmoidal curve of the velocity-pCa relationship, changes in Ca^{2+}-sensitivity and RTF cooperativity could become detectable even at extremely low pH levels. Interestingly, P_i has been shown to increase the unloaded velocity of RTFs in IVM and could be used to sample at low pH by providing a significant increase in velocity (13).

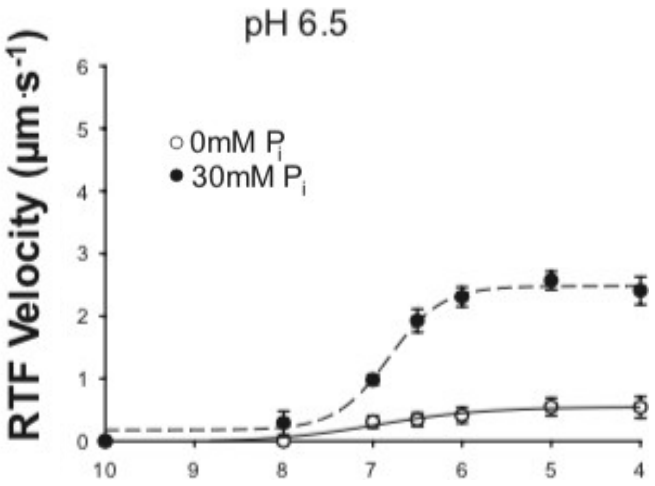

Figure 5.7: P_i recovers velocity in IVM at low pH and could be used to help experiment with lower pH levels by increasing velocity at most Ca^{2+} levels. From Debold et al. 2012.

A caveat of sampling in a combination of low pH and high P_i would be the inherent change in the type of experiment being conducted. The addition of P_i would not allow us to answer our original research question about defining the role that Tm has in acidosis as these new results would be confounded by the presence of P_i, and we would be unable to definitively attribute any results solely to the effects of acidosis.

In order to align experimental goals to solely investigating the effects of pH, another possibility that could increase IVM velocity at low pH would be with the incorporation of dATP (deoxyadenosine triphosphate). dATP has been shown to increase the rate of the cross-bridge cycle and the velocity of IVM (65) and could provide the increase in velocity needed to study Tm function during extreme acidosis.

BIBLIOGRAPHY

1. **Allen DG**, **Lamb GD**, **Westerblad H**. Impaired calcium release during fatigue. *J Appl Physiol Bethesda Md 1985* 104: 296–305, 2008.

2. **Barnard EA**, **Lyles JM**, **Pizzey JA**. Fibre types in chicken skeletal muscles and their changes in muscular dystrophy. *J Physiol* 331: 333-354.6, 1982.

3. **Brown JH**, **Cohen C**. Regulation of muscle contraction by tropomyosin and troponin: how structure illuminates function. *Adv Protein Chem* 71: 121–159, 2005.

4. **Broxterman RM**, **Layec G**, **Hureau TJ**, **Amann M**, **Richardson RS**. Skeletal muscle bioenergetics during all-out exercise: mechanistic insight into the oxygen uptake slow component and neuromuscular fatigue. *J Appl Physiol* 122: 1208–1217, 2017.

5. **Cady EB**, **Jones DA**, **Lynn J**, **Newham DJ**. Changes in force and intracellular metabolites during fatigue of human skeletal muscle. *J Physiol* 418: 311–325, 1989.

6. **Cooke R**, **Franks K**, **Luciani GB**, **Pate E**. The inhibition of rabbit skeletal muscle contraction by hydrogen ions and phosphate. *J Physiol* 395: 77–97, 1988.

7. **Cummins P**, **Perry SV**. The subunits and biological activity of polymorphic forms of tropomyosin. *Biochem J* 133: 765–777, 1973.

8. **Dean R. Appling**, **Spencer J. Anthony-Cahill**, **Christopher K. Mathews**. *Biochemistry: Concepts and Connections*. Pearson, 2016.

9. **Debold EP**. Recent insights into the molecular basis of muscular fatigue. *Med Sci Sports Exerc* 44: 1440–1452, 2012.

10. **Debold EP**. Decreased Myofilament Calcium Sensitivity Plays a Significant Role in Muscle Fatigue. *Exerc Sport Sci Rev* 44: 144–149, 2016.

11. **Debold EP**, **Beck SE**, **Warshaw DM**. Effect of low pH on single skeletal muscle myosin mechanics and kinetics. *Am J Physiol-Cell Physiol* 295: C173–C179, 2008.

12. **Debold EP**, **Fitts RH**, **Sundberg CW**, **Nosek TM**. Muscle Fatigue from the Perspective of a Single Crossbridge. *Med Sci Sports Exerc* 48: 2270–2280, 2016.

13. **Debold EP**, **Longyear TJ**, **Turner MA**. The effects of phosphate and acidosis on regulated thin-filament velocity in an in vitro motility assay. *J Appl Physiol Bethesda Md 1985* 113: 1413–1422, 2012.

14. **Debold EP**, **Turner MA**, **Stout JC**, **Walcott S**. Phosphate enhances myosin-powered actin filament velocity under acidic conditions in a motility assay. *Am J Physiol Regul Integr Comp Physiol* 300: R1401-1408, 2011.

15. **Eckhardt AL**, **Devon HA**, **Piano MR**, **Ryan CJ**, **Zerwic JJ**. Fatigue in the Presence of Coronary Heart Disease. *Nurs Res* 63: 83–93, 2014.

16. **Ekmann A**, **Osler M**, **Avlund K**. The predictive value of fatigue for nonfatal ischemic heart disease and all-cause mortality. *Psychosom Med* 74: 464–470, 2012.

17. **Fabiato A**, **Fabiato F**. Effects of pH on the myofilaments and the sarcoplasmic reticulum of skinned cells from cardiace and skeletal muscles. *J Physiol* 276: 233–255, 1978.

18. **Faul F**, **Erdfelder E**, **Lang A-G**, **Buchner A**. G*Power 3: A flexible statistical power analysis program for the social, behavioral, and biomedical sciences. *Behav Res Methods* 39: 175-191, 2007.

19. **Fitts RH**. Cellular mechanisms of muscle fatigue. *Physiol Rev* 74: 49–94, 1994.

20. **Fujita H**, **Ishiwata S**. Tropomyosin modulates pH dependence of isometric tension. *Biophys J* 77: 1540–1546, 1999.

21. **Fukuda N**, **O-Uchi J**, **Sasaki D**, **Kajiwara H**, **Ishiwata S**, **Kurihara S**. Acidosis or inorganic phosphate enhances the length dependence of tension in rat skinned cardiac muscle. *J Physiol* 536: 153–160, 2001.

22. **Gordon AM**, **Huxley AF**, **Julian FJ**. The variation in isometric tension with sarcomere length in vertebrate muscle fibres. *J Physiol* 184: 170–192, 1966.

23. **Gordon AM**, **Regnier M**, **Homsher E**. Skeletal and Cardiac Muscle Contractile Activation: Tropomyosin "Rocks and Rolls." *Physiology* 16: 49–55, 2001.

24. **Greenberg MJ**, **Moore JR**. The molecular basis of frictional loads in the in vitro motility assay with applications to the study of the loaded mechanochemistry of molecular motors. *Cytoskeleton* 67: 273–285, 2010.

25. **Greenfield NJ**, **Huang YJ**, **Swapna GVT**, **Bhattacharya A**, **Rapp B**, **Singh A**, **Montelione GT**, **Hitchcock-DeGregori SE**. Solution NMR Structure of the Junction between Tropomyosin Molecules: Implications for Actin Binding and Regulation. *J Mol Biol* 364: 80–96, 2006.

26. **Heller MJ**, **Nili M**, **Homsher E**, **Tobacman LS**. Cardiomyopathic tropomyosin mutations that increase thin filament Ca2+ sensitivity and tropomyosin N-domain flexibility. *J Biol Chem* 278: 41742–41748, 2003.

27. **Holmes KC**, **Lehman W**. Gestalt-binding of tropomyosin to actin filaments. *J Muscle Res Cell Motil* 29: 213–219, 2008.

28. **Holthauzen LMF**, **Corrêa F**, **Farah CS**. Ca2+-induced Rolling of Tropomyosin in Muscle Thin Filaments THE α- AND ß-BAND HYPOTHESIS REVISITED. *J Biol Chem* 279: 15204–15213, 2004.

29. **Homsher E**, **Kim B**, **Bobkova A**, **Tobacman LS**. Calcium regulation of thin filament movement in an in vitro motility assay. *Biophys J* 70: 1881–1892, 1996.

30. **Homsher E**, **Lee DM**, **Morris C**, **Pavlov D**, **Tobacman LS**. Regulation of force and unloaded sliding speed in single thin filaments: effects of regulatory proteins and calcium. *J Physiol* 524: 233–243, 2000.

31. **Homsher E**, **Nili M**, **Chen IY**, **Tobacman LS**. Regulatory proteins alter nucleotide binding to acto-myosin of sliding filaments in motility assays. *Biophys J* 85: 1046–1052, 2003.

32. **Huxley AF**. Muscle structure and theories of contraction. *Prog Biophys Biophys Chem* 7: 255–318, 1957.

33. **Huxley HE**. Sliding filaments and molecular motile systems. *J Biol Chem* 265: 8347–8350, 1990.

34. **Joyner MJ**, **Coyle EF**. Endurance exercise performance: the physiology of champions. *J Physiol* 586: 35–44, 2008.

35. **Karabina A**, **Kazmierczak K**, **Szczesna-Cordary D**, **Moore JR**. Myosin regulatory light chain phosphorylation enhances cardiac β-myosin in vitro motility under load. *Arch Biochem Biophys* 580: 14–21, 2015.

36. **Kent-Braun JA**. Central and peripheral contributions to muscle fatigue in humans during sustained maximal effort. *Eur J Appl Physiol* 80: 57–63, 1999.

37. **Kent-Braun JA**, **Fitts RH**, **Christie A**. Skeletal muscle fatigue. *Compr Physiol* 2: 997–1044, 2012.

38. **Kent-Braun JA**, **Ng AV**, **Doyle JW**, **Towse TF**. Human skeletal muscle responses vary with age and gender during fatigue due to incremental isometric exercise. *J Appl Physiol Bethesda Md 1985* 93: 1813–1823, 2002.

39. **Knuth ST**, **Dave H**, **Peters JR**, **Fitts RH**. Low cell pH depresses peak power in rat skeletal muscle fibres at both 30 degrees C and 15 degrees C: implications for muscle fatigue. *J Physiol* 575: 887–899, 2006.

40. **Kron SJ**, **Spudich JA**. Fluorescent actin filaments move on myosin fixed to a glass surface. *Proc Natl Acad Sci U S A* 83: 6272–6276, 1986.

41. **Lehman W**, **Li X**, **Kiani FA**, **Moore JR**, **Campbell SG**, **Fischer S**, **Rynkiewicz MJ**. Precise Binding of Tropomyosin on Actin Involves Sequence-Dependent Variance in Coiled-Coil Twisting. *Biophys J* 115: 1082–1092, 2018.

42. **Lehman W**, **Medlock G**, **Li X (Edward)**, **Suphamungmee W**, **Tu A-Y**, **Schmidtmann A**, **Ujfalusi Z**, **Fischer S**, **Moore JR**, **Geeves MA**, **Regnier M**. Phosphorylation of Ser283

enhances the stiffness of the tropomyosin head-to-tail overlap domain. *Arch Biochem Biophys* 571: 10–15, 2015.

43. **Lewis WG**, **Smillie LB**. The amino acid sequence of rabbit cardiac tropomyosin. *J Biol Chem* 255: 6854–6859, 1980.

44. **Li XE**, **Holmes KC**, **Lehman W**, **Jung H**, **Fischer S**. The shape and flexibility of tropomyosin coiled coils: implications for actin filament assembly and regulation. *J Mol Biol* 395: 327–339, 2010.

45. **Li XE**, **Tobacman LS**, **Mun JY**, **Craig R**, **Fischer S**, **Lehman W**. Tropomyosin position on F-actin revealed by EM reconstruction and computational chemistry. *Biophys J* 100: 1005–1013, 2011.

46. **Longyear T**, **Walcott S**, **Debold EP**. The molecular basis of thin filament activation: from single molecule to muscle. *Sci Rep* 7: 1822, 2017.

47. **Mak AS**, **Smillie LB**, **Stewart GR**. A comparison of the amino acid sequences of rabbit skeletal muscle alpha- and beta-tropomyosins. *J Biol Chem* 255: 3647–3655, 1980.

48. **Margossian SS**, **Lowey S**. Preparation of myosin and its subfragments from rabbit skeletal muscle. *Methods Enzymol* 85 Pt B: 55–71, 1982.

49. **McKillop DF**, **Geeves MA**. Regulation of the interaction between actin and myosin subfragment 1: evidence for three states of the thin filament. *Biophys J* 65: 693–701, 1993.

50. **McLachlan AD**, **Stewart M**. The 14-fold periodicity in α-tropomyosin and the interaction with actin. *J Mol Biol* 103: 271–298, 1976.

51. **Memo M**, **Marston S**. Skeletal muscle myopathy mutations at the actin tropomyosin interface that cause gain- or loss-of-function. *J Muscle Res Cell Motil* 34: 165–169, 2013.

52. **Merton PA**. Voluntary strength and fatigue. *J Physiol* 123: 553–564, 1954.

53. **Monteiro PB**, **Lataro RC**, **Ferro JA**, **Reinach F de C**. Functional alpha-tropomyosin produced in Escherichia coli. A dipeptide extension can substitute the amino-terminal acetyl group. *J Biol Chem* 269: 10461–10466, 1994.

54. **Moore JR**, **Campbell SG**, **Lehman W**. Structural determinants of muscle thin filament cooperativity. *Arch Biochem Biophys* 594: 8–17, 2016.

55. **Moore JR**, **Prum T**, **Fagnant PM**, **Trybus KM**, **Lehman W**. D292V Actin Mutation Stabilizes Tropomyosin in the Off-State of the Thin Filament. *Biophys J* 112: 259a, 2017.

56. **Mozaffarian D**, **Benjamin EJ**, **Go AS**, **Arnett DK**, **Blaha MJ**, **Cushman M**, **de Ferranti S**, **Després J-P**, **Fullerton HJ**, **Howard VJ**, **Huffman MD**, **Judd SE**, **Kissela BM**, **Lackland DT**,

Lichtman JH, **Lisabeth LD**, **Liu S**, **Mackey RH**, **Matchar DB**, **McGuire DK**, **Mohler ER**, **Moy CS**, **Muntner P**, **Mussolino ME**, **Nasir K**, **Neumar RW**, **Nichol G**, **Palaniappan L**, **Pandey DK**, **Reeves MJ**, **Rodriguez CJ**, **Sorlie PD**, **Stein J**, **Towfighi A**, **Turan TN**, **Virani SS**, **Willey JZ**, **Woo D**, **Yeh RW**, **Turner MB**, **American Heart Association Statistics Committee and Stroke Statistics Subcommittee**. Heart disease and stroke statistics--2015 update: a report from the American Heart Association. *Circulation* 131: e29-322, 2015.

57. **Nelson CR**, **Debold EP**, **Fitts RH**. Phosphate and acidosis act synergistically to depress peak power in rat muscle fibers. *Am J Physiol Cell Physiol* 307: C939-950, 2014.

58. **Okita K**, **Kinugawa S**, **Tsutsui H**. Exercise intolerance in chronic heart failure--skeletal muscle dysfunction and potential therapies. *Circ J Off J Jpn Circ Soc* 77: 293–300, 2013.

59. **Orzechowski M**, **Moore JR**, **Fischer S**, **Lehman W**. Tropomyosin movement on F-actin during muscle activation explained by energy landscapes. *Arch Biochem Biophys* 545: 63-68, 2014.

60. **Pardee JD**, **Spudich JA**. Purification of muscle actin. *Methods Enzymol* 85 Pt B: 164–181, 1982.

61. **Parsons B**, **Szczesna D**, **Zhao J**, **Van Slooten G**, **Kerrick WG**, **Putkey JA**, **Potter JD**. The effect of pH on the Ca2+ affinity of the Ca2+ regulatory sites of skeletal and cardiac troponin C in skinned muscle fibres. *J Muscle Res Cell Motil* 18: 599–609, 1997.

62. **Paulucci AA**, **Hicks L**, **Machado A**, **Miranda MTM**, **Kay CM**, **Farah CS**. Specific sequences determine the stability and cooperativity of folding of the C-terminal half of tropomyosin. *J Biol Chem* 277: 39574–39584, 2002.

63. **Perry SV**. Vertebrate tropomyosin: distribution, properties and function. *J Muscle Res Cell Motil* 22: 5–49, 2001.

64. **Redwood C**, **Robinson P**. Alpha-tropomyosin mutations in inherited cardiomyopathies. *J Muscle Res Cell Motil* 34: 285–294, 2013.

65. **Regnier M**, **Rivera AJ**, **Chen Y**, **Chase PB**. 2-deoxy-ATP enhances contractility of rat cardiac muscle. *Circ Res* 86: 1211–1217, 2000.

66. **Risi C**, **Eisner J**, **Belknap B**, **Heeley DH**, **White HD**, **Schröder GF**, **Galkin VE**. Ca2+-induced movement of tropomyosin on native cardiac thin filaments revealed by cryoelectron microscopy. *Proc Natl Acad Sci* 114: 6782–6787, 2017.

67. **Robergs RA**, **Ghiasvand F**, **Parker D**. Biochemistry of exercise-induced metabolic acidosis. *Am J Physiol Regul Integr Comp Physiol* 287: R502-516, 2004.

68. **Sata M**, **Sugiura S**, **Yamashita H**, **Fujita H**, **Momomura S**, **Serizawa T**. MCI-154 Increases Ca2+ Sensitivity of Reconstituted Thin Filament [Online]. *Circ. Res.* https://www.ahajournals.org/doi/abs/10.1161/01.res.76.4.626 [3 Oct. 2018].

69. **Sata M**, **Yamashita H**, **Sugiura S**, **Fujita H**, **Momomura S -ichi**, **Serizawa T**. A new in vitro motility assay technique to evaluate calcium sensitivity of the cardiac contractile proteins. *Pflüg Arch* 429: 443–445, 1995.

70. **Stone D**, **Smillie LB**. The amino acid sequence of rabbit skeletal alpha-tropomyosin. The NH2-terminal half and complete sequence. *J Biol Chem* 253: 1137–1148, 1978.

71. **Tanaka H**. The helix content of tropomyosin and the interaction between tropomyosin and F-actin under various conditions. *Biochim Biophys Acta* 278: 556–566, 1972.

72. **Thedinga E**, **Karim N**, **Kraft T**, **Brenner B**. A single-®ber in vitro motility assay. In vitro sliding velocity of F-actin vs. unloaded shortening velocity in skinned muscle ®bers. .

73. **VanBuren P**, **Palmiter KA**, **Warshaw DM**. Tropomyosin directly modulates actomyosin mechanical performance at the level of a single actin filament. *Proc Natl Acad Sci U S A* 96: 12488–12493, 1999.